

Point-to-point Response to the comments:

Response to reviewers' comments on the manuscript angeo-2018-131-RC1: Spatial gradient of total electron content (TEC) between two nearby stations as indicator of occurrence of ionospheric irregularity

Authors: Teshome Dugassa, John Bosco Habarulema, and Melessew Nigussie

General remarks

We thank the two referees for their comments and suggestions which have led to an improved, revised manuscript. Those comments are all valuable and very helpful for revising and improving our paper, as well as the important guiding significance to our research. We have reacted to the comments carefully and have made correction which we hope meet with approval. We revised the introduction. We added graphs and discussions. The responds to the comments are as flowing:

Referee #1

General comments

1. **The study attempts to show how the difference between the TEC of two close GNSS stations can be used as a precursor of ionospheric irregularities in the post sunset period over both stations. The study being the first of its kind in the African sector is worthy of interest couple with the fact that it is well written and it gives insight about a possible relation between electric field and irregularities in the post sunset period. However, the authors first need to give a good justification why they want to use TEC gradient between two stations as a proxy of irregularities.**

Response:

Yes, it's a good comment. We have revised the introduction of the manuscript and added the justification why we used TEC gradient between two nearby located stations as indicator of occurrence of ionospheric irregularities (**Page 2: Lines 23-34 and Page 3: Lines 1-33**).

Previous studies explained the relation between the latitudinal (N-S) gradient of TEC surrounding the anomaly region and ionospheric scintillation over different sectors (Muella et al., 2008). Even though, the characteristics of ionospheric irregularities/plasma bubbles over equatorial/low-latitude region of Africa under different solar and geomagnetic activities were discussed Mungufeni et al. (2016), a limited number of studies have been carried out over the region relating the latitudinal/longitudinal gradient of TEC/plasma density and the occurrence of ionospheric irregularities.

The longitudinal gradient of integrated Pederson conductivity in the E-region at sunset time play a fundamental role in the strengthening the PRE magnitude and affect the generation of ionospheric irregularities (Tsumoda, 1985). It is well known that PRE is a postsunset phenomena which uplift the ionosphere and create a conducive condition for irregularity formation. This implies the magnitude of the zonal electric field is an important parameter for real-time prediction. It is also known that PRE is due to spatial gradient of electron density near solar-terminator. However, it is not easy to obtain the longitudinal gradient of electron density over Africa longitude sector as ionosondes are not available in nearby locations and study the relationship between the electron density gradient and occurrence of ionospheric irregularities. We know TEC is the integral of electron density, so a closely located GPS receivers would help us to estimate the strength of the zonal electric field and investigate the relation between the gradient of TEC and occurrence of irregularities.

2. **Giving the fact that ROTI which can be easily estimated is already an indicator of irregularities why use the gradient between two stations to do the same work?**

Response:

It is well known that ROTI is a proxy for the occurrence of ionospheric irregularities and scintillations. From the definition, however, ROTI mixes both the spatial and temporal gradients of TEC variations. The relationship between the spatial gradient of TEC and ROTI was established to observe how the gradient of TEC affect radio signals, presents information that the horizontal electron density gradient as an important parameter to predict ionospheric scintillation. After establishing this relationship showing that both parameters give information about ionospheric irregularities, TEC gradient method may be an alternative as it is a simple computation of establishing the difference (**Page 3: Lines 6-33**).

3. **What if the constraints “over the same latitude, but separated by a longitudinal of about 5 degree” is removed? What happens to the relation?**

Response:

We thank the reviewer for the important point raised. We have a plan to investigate the optimum separation between two GNSS receivers that can provide the best correlation between TEC gradient and irregularity. This will be done in a separate work.

Specific comments

1. **How does the relationship between TEC gradient and ROTI is established? The study never really specified or took into consideration the quietness and/or disturbed nature of the days used.**

Response:

Thank you for your good suggestions. To show the relationship between the TEC gradient and ROTI, the 10 quiet international days in the year 2014 were used. In this study period, there are about 364 days fully available in both stations simultaneously. The quiet international days are obtained from <http://wdc.kugi.kyoto-u.ac.jp/qddays/index.html>. In total, about 120 quiet days were used in investigating the relationship between TEC gradient and ROTI. The maximum value of the standard deviation of the spatial gradient of TEC was used to observe the correlation between the gradient of TEC and ROTI (**Page 18, Figure 8**). Moreover, in the revised version of the manuscript, disturbed days were also examined. (**Page 15, Figure 5**).

2. **In establishing a relation between equatorial electric field and spatial gradient, the authors used only four days in year 2014. Is this sufficient enough to show any kind of relationship between both quantities?**

Response:

In the previous version of the manuscript, we used four quiet days as a typical example to observe a relation between equatorial electric field and spatial gradient of TEC which is not sufficient enough. In the revised version of the manuscript, however, we modified Figure 2 by adding more data/months to establish the relationship between the equatorial electric field and spatial gradient. In the updated graphs, we took the monthly-quiet mean of the equatorial electric field and TEC gradient of the year 2014 (**Page 11, Figure 2**).

3. **In Justifying the magnetic data gap (the H component of the Earth’s magnetic field) in 2014, the authors performed a correlation between the equatorial electrojet ΔH and equatorial electric field (EEF) for quiet days in 2012. No information is given on these days and how they were selected and how many they are?**

Response:

Five quietest international days of each month of the year 2014 were utilized to perform the correlation between the equatorial electrojet ΔH and the equatorial electric field (EEF). These days are obtained from http://isgi.unistra.fr/data_download.php. Out of 60 days, only 38 days of data were available simultaneously in both magnetometer measuring stations (**Page 9, Figure 1b**).

4. **The authors assumed the correlation between ΔH and EEF as obtained in 2012 (0.7) will be the same in 2014.**

Response:

We did the correlation between ΔH and EEF to justify the performance and reliability of the model over the equatorial region of Africa using available magnetometer data (the year 2012). As can be seen from their relation, the day time EEF model and day time ΔH correlated positively. Since the performance of the model was good, we could use the real-time electric field model for the year 2014 in the absence of ΔH data to observed the possible relation between electric field and irregularities/TEC gradient in the post-sunset period. Actually, the two selected years have a different solar condition. However, the average value of F10.7cm for the quiet days in the two years does not show significant variation (**Page 9, Figure 1b**).

Listing of technical corrections

Abstract

1. **Line 9: Change correlation to relation. I did not see any correlation study between both variables in this work.**

Response: As suggested, we have changed the term “correlation” to “relationship” (**Page 1, Line 13**).

2. **Line 11: Maximum positive/depletions. Why not use maximum enhancement and reduction. The spatial gradient will either be positive or negative. A negative gradient means reduction in electron density. Let’s avoid using the word depletion since it can be mistaken for TEC depletion.**

Response: Ok, we replaced (Words and phrases stated maximum positive/depletions was corrected to maximum enhancement and reduction). (**Page 1, Line 7, 16**).

3. **Line 15-16: The spatial gradient of TEC between the two nearby stations could be used as an indicator of the occurrence of ionospheric irregularities. Is it over both stations or it is a general statement?**

Response: Over both stations (We did correlation for both stations) (**Page 1, Line 13 - 15**).

Introduction

Page 2

4. **Line 8: Attests**

Response: Modified.

5. **Line 14. Remove mechanism**

Response: Corrected (**Page 2, Line 11**).

6. **Line 18. ESF write in full. First time used.**

Response: We accept it and corrected in the revised manuscript (**Page 2, Line 25**).

7. **Line 30. GPS write in full. The GPS scintillation index, S4 is not an instrument. The GPS is.**

Response: We accept it and corrected in the revised manuscript (**Page 3 , Line 12**).

8. **Line 31. Global Navigation Satellite System (GNSS). Use either GNSS or GPS.**

Response: We accept it and corrected in revised manuscript (**Page 1, Line 5, 19**).

Page 3

9. **From lines 1-2, a mention of some work done over Africa has been made. However nothing was said about the scope of such studies, their limitations/gaps and how they relate to this study. Kindly address.**

Response: It is a good suggestion, the limitations/gaps of the previous study that has been done over Africa equatorial/low-latitude region and how the current study related to this study was discussed (**Page 3 Lines 6-20**).

10. **Line 26. "and see". Change to as well as study.**

Response: Modified.

11. **Line 27 "A closely found" change to closely located**

Response: corrected (**Page 3, Line 23**).

12. **Line 28. I am not comfortable with the word 'longitudinal'. Change to spatial for uniformity with title.**

Response: As suggested we changed 'longitudinal' to 'Spatial' (**Page 3, Line 29**).

13. **Line 27-28. What is the justification for the study of the relation between longitudinal (in this case spatial) gradient of TEC derived from two GPS receivers and occurrence of ionospheric irregularities still using GPS?**

Response: Modified (**Page 2, 23-35, Page 3 Lines 21-29,)**

14. **Line 29. Same as in line 28.**

Response: Corrected.

Page 4

Data and methods

15. **Line 2-3: Kindly read that statements and adjust for easy flow.**

Response: It is a good suggestions. We adjust the statement for easy flow (**Page 4, Lines 4-13**).

16. **Line 5: Why 2014 only? Is there any particular justification for th choice of this year?**

Response: It is because this year had sufficient simultaneous data for both stations for statistical values to be reliable.

17. **Line 6: Remove "of"**

Response: We corrected it as suggested.

18. **Lines 7-8: Change the first average to "mean".**

Response: As suggested we changed the "average" to "mean".

19. **Line 10: change were to "was".**

Response: We corrected.

20. **Line 10: "then analyzed to show the possible indicator of". This statement is not correct. Adjust**

Response: We adjusted the statement.

21. **Line 11:** "The spatial gradient of TEC between the two nearby stations are located nearly along the same". Adjust statement. May be you should delete "are".

Response: Corrected.

22. **Line 14:** Any reference for equation 1?

Response: Yes, we have references for the equation (Page 4, Line 26).

23. **Line 16-17:** I am not satisfied with your definition of ΔH the way it is and the way you associate it to the EEJ in these particular lines. In addition you need to add how the H was processed and corrected for baseline value and non cyclic variations.

Response: Yes, it is a good suggestion. In the revised manuscript we modified how H was processed (Page 5, 6, and 7).

24. **Line 22:** ...is a transfer function model which to models the daily variations. . . Check the sentence.

Response: The sentence was modified.

Page 5

25. **Line 1:** "which are mapped from interplanetary electric field (IEF) data". Change to ... which are mapped in the interplanetary electric field (IEF).

Response: corrected.

26. **Line 5:** I think you need to clearly explain the various options that the model provides and then proceed to tell us exactly which of the three options you used and why.

Response: corrected.

27. **Line 16:** add "s" to station.

Response: Corrected.

28. **Line 23:** Put a comma after reliable.

Response: Corrected.

29. **Line 24:** Change "from the model" to 'it'

Response: As suggested we changed "from the model" to 'it' in the revised manuscript.

30. **Line 32:** Was ROTI introduced to quantify the ROT measurements or ionospheric irregularities? Clarify please.

Response: It is a good comment. We clarified what ROTI indicates.

Page 6

31. **Line 6:** Adjust to (Ma and Maruyama, 2006).

Response: As suggested we adjusted the way we cited the authors.

32. **Line 23:** I thought the scope of the study was 2014. Why use data from 2012? Have you accounted for the yearly variation and solar activity influence in juxtaposing your 2012 and 2014 data? Please could you clarify this?

Response:

Since magnetometer data during the year 2012 was available simultaneously both at dip equator (Addis Ababa)

and off-equator (Adigrat) we used these data to observe the performance of equatorial electric field model over equatorial region of Africa. The model correlates moderately over equatorial region of Africa, and hence we used the model over the region, during the year 2014 (Page: 7-8).

Results and Discussions

33. Line 22: For some of selected. Remove of

Response: We accept it and corrected in the revised manuscript

34. Lines 22-23. How did you select those quiet days? How many where there? What is the temporal resolution of both ΔH and EEF. Is the correlation obtained from "some selected quiet days" be an adequate representation of all other quiet days in year 2012? Check Figure caption in Figure 1 and harmonize. Let's know whether you use some days or quiet days of month of year 2012.

Response:

The quiet days used in this study are the international five quiet days of each month of year 2014 obtained from Kyoto website. Only 38 quiet days available. The temporal resolution of ΔH is 1 min and EEF is 5 min. We corrected the resolution of ΔH to 5 min resolution. We modified the correlation between the EEF and ΔH using the quiet days of year 2012. The graph is replotted. Caption of Figure 1 is also modified (Page 9, Figure 1).

Page 7

35. Lines 2-5. You gave us a beautiful description of how ΔH can be derived between the two magnetometers just for you to come and tell us that the data were not available for year 2014. I think it should have been the other way round.

Response: The interest of showing the relationship between ΔH derived between the magnetometers and EEF derived from equatorial electric field model for the year 2014 was described in the revised manuscript.

36. Line 3. Correct Adegrat to Adigrat.

Response: As suggested, we have corrected "Adegrat" to "Adigrat".

37. Line 4-5. To solve this data gap we used the daytime information of equatorial electric field derived from the real-time prompt penetration electric field model as an option. Did you use the real time model of Ionospheric electric fields of the real-time prompt penetration electric field model?

Response: We have used the real time model of Ionospheric electric fields of the real-time prompt penetration electric field model.

38. In Page 6 lines 21-23 the authors claimed the relation is for some selected quiet days of months of year 2012 but in Page 7, lines 5-7 they state that the same relation is for year 2012. This may be extremely misleading.

Response: Yes, it is a good suggestion. To show the relationship between ΔH and EEF, we update the considered days by considering the international quietest days of months of year 2012.

39. We need a clear explanation on how you wish to use correlation result for 2012 to support some of your results in 2014. You must be aware of the solar activity influence on vertical drift. It will not be totally accurate to say that the correlation in 2012 will be the same as those in 2014. May be you did that as an indication of something. You need to clarify.

Response:

The correlation between the equatorial electric field model and ΔH in the year 2012 was made to observe the

performance of the model over the equatorial region of Africa, East Africa. We choice the year 2012 just because of availability of magnetometer data at both stations (Addis Ababa and Adigrat). The performance of the model over this sector was moderate ($C = 0.6$).

Page 8

40. **Line 5: Be consistent. Is it Figure or Fig? (check in all texts and harmonize).**

Response: We used Figure/Fig ways in referring figures according to the style of the journal.

41. **Line 7. Replace “but lags’ with “ but after ‘?..**

Response: We accept it and corrected in the revised manuscript.

42. **Line 8: The depletions in the gradient. I am not comfortable with the word depletion. Kindly use the reduction in the gradient.**

Response: As suggested we replaced “depletions in the gradient” by “reduction in the gradient” a new in new manuscript.

43. **Line 9: ...maximum positive of the spatial gradient of ... Replace with “ the peak of spatial gradient” or “the maximum spatial gradient”.**

Response: As suggested we replaced “maximum positive of the spatial gradient” by “the maximum spatial gradient” a new in new manuscript.

44. **Line 11: Change depletion with reduction.**

Response: As suggested, we replaced it.

45. **Lines 16-19: Why over Asab only?**

Response: Graph of Debark also added (**Page 11-12, 14-19, Figure 2-9**).

Page 9

46. **30 March 2014, 10 April 2014, 20 September 2014, 10 October 2014. Where these days selected randomly?**

Response:

Over equatorial/low-latitude regions of Africa, since a high rate of occurrence of irregularities observed in the equinoctial seasons, and we selected the equinoctial seasons of the year 2014. And, these days are quiet days of the selected months.

47. **The caption in Figure 3 should be self explanatory and should tell us the stations (Asab and Debark) that were used for the ROTI.**

Response: It is a good comment. We modified the caption of Figure 3 (**Page 12, Figure 3**).

Page 10

48. **Line 1: Do you have any reference for this?**

Response: Yes (**Page 11, Line 32**).

49. **Line 1: From the figure, ... Which Figure? Specify.**

Response: We specified the referred figure in the revised manuscript.

50. **Lines 2-3: A convincing and quantitative way to demonstrate inferences in lines 3-4 is by performing correlation between spatial gradient and irregularities.**
Response: The graph was modified and replotted (Page 18, Figure 8).
51. **Lines 7-8: An ionosphere gradient of 518 mm/km was discovered, generated by a plasma bubble. Read the statement and rephrase.**
Response: The statement was rephrased in the revised manuscript.
52. **Line 14: (see., Fig. 5). Change to as seen in Figure 5.**
Response: As suggested we have changed “Change” to “as seen”.
53. **Line 17: Change “a” by “the”**
Response: We changed “a” by “the” as suggested.
54. **Line 18: Change “indicates” to “shows”**
Response: We have changed the phrase as suggested.
55. **Line 19: ...in section (2)... which section 2? Change to as stated earlier.**
Response: Thank you. We have changed the phrase as suggested.
56. **Line 23: Put ‘s’ to period**
Response: corrected.
57. **Line 23-24: Equation (1) was applied to all days of the year 2014? Including disturbed days? This is where it is important to separate disturbed days from quiet ones. We know that gradients can be significant during geomagnetic storms.**
Response: The correlation between the TEC gradient and ROTI was done only for the quiet days (Page 12, Figure 3; Page 18, Figure 8).
58. **Line 28 - 32: Most of the observed features have not been discussed and plausible answers not given to explain them.**
Response: Thank you for your good suggestions. The observed features of results are discussed (Page 11, Lines 1-35, Page 16, Lines 1-16).
59. **Line 32: Change depletions to reductions.**
Response: As suggested, we changed “depletion” to “reduction”.
60. **Figure 4: a) Diurnal variation of the spatial gradient of TEC over ASAB and DEBK , b) Daily maximum value of the spatial gradient of TEC variation, c) Diurnal variation of ROTIave over ASAB station and d) Daily maximum value variation of ROTIaave over ASAB station in the year 2014. Check this Figure caption and adjust according to your Figures (e) and (f) are missing.**
Response: It is a good comment. The caption of the figures are adjusted and replotted (Page 16, Figure 6).
- Page 11
61. **Lines 1-2. If you can show it don’t say it.**
Response:: Yes, we adjusted the statement .

62. **Lines 10-11. “The trend they show has similarity with” The trend is already a similarity. Adjust the statement.**

Response: The statement is adjusted.

63. **The caption of Figure 4 is misleading. Please check and let it conform with what you have in the texts.**

Response: It is a good comment. The caption of the figure is modified (**Page 16, Figure 6**).

64. **Why not add a correlation plot between spatial gradient and ROTI over each station? This is a better way of obtaining quantitative information between both quantities.**

Response: Yes, it’s a good suggestion. The relationship between spatial gradient and ROTI over each stations were illustrated by showing the correlation between them (**Page 18, Figure 8**).

Page 12

65. **Line 3: What about Debark? Why is it not presented? Besides, is this Figure for quiet and disturbed periods? How did you segregate the effect of transient disturbances?**

Response:

Percentage of occurrence of ionospheric irregularities for Debark is plotted (**Page 20, Figure 9**). The figures are both for quiet and disturbed periods. We didn’t segregate the effect of transient disturbances, since it is not the objective of the study. This may be worked in the future.

66. **Line 26: Basu et al., the year is missing.**

Response: We corrected the missed part of the cited reference.

Page 13

67. **Line 6: Change “has not been seen” to something suitable.**

Response: Modified.

Page 14

Conclusions

68. **Lines 2-3: This is inconclusive and cannot feature in this section given the fact the relation between EEF and TEC gradient was investigated for just for 4 days (Figure 2).**

Response: Well, we update Figure 2 of the previous version of the manuscript. Graphs of quiet-monthly mean of each month of year 2014 for both EEF and TEC gradient was plotted to observe features showing the relation between EEF and TEC gradient (**Page 11, Figure 2**).

Acknowledgments

69. **Line 6: Remove and.**

Response: corrected.

70. **Lines 7-8: We acknowledge <http://www.geomag.org/models/PPEFM/RealtimeEF.html> for providing the data the Prompt penetration equatorial electric field model. Give proper acknowledgement please.**

Response: Thank you very much. We update the acknowledgement of the manuscript (**Page 21**).

71. **Line 8: Provide adequate acknowledgement for using the AMBER data (Visit AMBER website for adequate acknowledgement).**

Response: Thank you for your good suggestion. We acknowledged adequately (**Page 21**).

References

Page 15

72. **Line 31-32: Incomplete reference.**

Response: Yes, it was incomplete. In the revised manuscript we completed the full information of the reference (**Page 22**).

Page 16

73. **Line 16-20: Arrange references chronologically.**

Response: We are using bibtex and the references are printed automatically. May be it is the style of the journal.

74. **Line 36: Adjust the initials.**

Response: Adjusted.

Page 17

75. **Line 1-5: Arrange references chronologically. Also consider the reference in P.16 line 36-37 in the chronological arrangement.**

Response: We are using bibtex and the references are printed automatically. May be it is the style of the journal.

Response to reviewers' comments on the manuscript angeo-2018-131-RC2: Spatial gradient of total electron content (TEC) between two nearby stations as indicator of occurrence of ionospheric irregularity

Referee #2

(a) **Figures 2 and 3 needs a bit more clarification. I understand that the blue curves in Figure 3 shows the spatial gradient and the blue curve in Figure 2 shows enhancement in spatial gradient. What does the authors mean by enhancement/depletion in spatial gradient? Please mention how the enhancement/depletion in spatial gradient is calculated in Figure 2. I am just confused if the blue line in Figure 2 represent spatial gradient in TEC or enhancement in spatial gradient in TEC. The two sentences in lines 3-4 on page 8 are confusing. Considering Figures 2 and 3 are the most important figures of this manuscript they must be explained properly.**

Response:

In both of the graphs (Figures 2 and 3), the blue curves show the diurnal variation in the gradient of TEC. In Figure 2, the authors try to relate the electric field derived from equatorial electric field model and the spatial gradient in TEC. Whereas, Figure 3 was presented to show the trends of the time variation of ROTI

and the gradient in TEC. In both figures, the maximum enhancement/reduction in the gradient of TEC was observed. **(Page 11 and 12, Figures 2 and 3)**

On the computation of the spatial gradient of TEC between the two nearby located stations (ASAB and DEBK), the gradient of TEC may be either positive/negative value. Both the negative and positive values obtained from the differences of TEC between the two stations show the gradient of TEC. It is obvious that the positive/negative gradient in TEC is obtained when the minuend is larger/smaller than the subtrahend. A positive gradient in TEC denotes a higher in TEC/electron density over ASAB relative to DEBK and a negative gradient in TEC indicates a lower in TEC/electron density over ASAB than DEBK, i.e, a higher in TEC/electron density over DEBK than ASAB.

In the manuscript, we have used the term maximum enhancement/reduction in the gradient of TEC (in terms of magnitude) when the nighttime value of gradient of TEC was larger than the daytime value. Since fluctuation in ionospheric plasma density was prevalent during the nighttime hours, we have used the state of the night time gradient of TEC compared to daytime to describe the relationship between the gradient in TEC and the occurrence ionospheric irregularities.

The authors modified the term enhancement/depletion in the spatial gradient of TEC to maximum enhancement/reduction in the gradient of TEC. In the current study, there was no quantitative method that we have used to calculate the maximum enhancement/reduction in the gradient of TEC. We rather described the state of the gradient of TEC (which shows maximum positive/negative in TEC/electron density during nighttime relative to the daytime) by observing the values of gradient of TEC. The gradient in TEC was calculated by taking the difference of TEC between two stations (ASAB and DEBK) and divided by their longitudinal differences. If the gradient of TEC during nighttime is positive/negative values, the state of gradient of TEC show enhancement/reduction in gradient of TEC.

- (b) **Page 8 Line # 9-10: The authors state: “The spatial gradient of TEC observed during the day time was relatively small compared to the evening time values for most of the days.” If you take a look at Figure 3c, the daytime peak and the post sunset peak of the spatial gradient are almost of same values.**

Response:

The statement was modified as, “most of the day time value of spatial gradient in TEC was relatively small in magnitude compared to the night values.”

- (c) **Also the authors need to explain what do the increase or decrease in the spatial gradient in TEC mean physically. For example, in case of ROTI, it is very straight forward. If you look at Figure 3, the day time ROTI stays around zero. Postsunset, the ROTI values increase showing fluctuations in TEC (hence density). In case of ROTI, a standard value of 0.5 is considered to identify ionospheric irregularities.**

However, in case of spatial gradient of TEC, you can see daytime fluctuations as well. So what you see postsunset, may not entirely be due to fluctuations in TEC or irregularities. It may have a significant contribution due to zonal plasma drift. How do you eliminate that possibility?

Response:

Thank you for the suggestion. In the manuscript we modified the term increase/decrease in the spatial gradient of TEC to maximum enhancement/reduction in the gradient of TEC.

At a basic level, there are two independent ways of estimating the TEC gradient values using ground based GPS receiver data (Lee et al., 2006). The first method uses a pair of closely-spaced receiver stations. The second method uses a single GPS receiver station to infer the spatial TEC gradient values based on the observed temporal rate of change in TEC. The two methods actually have their own merit and demerits.

In our study, we have used the first method (i.e., station-pair method). This station-pair method gives us an instantaneous estimate of the TEC gradient along a fixed direction determined by the line segment connecting the two stations. It is true that the zonal drift might have an effect on TEC gradient. As the two stations used to get TEC gradient are close to each other, the same irregularity have a chance to be observed at these stations almost at the same time and hence difference of TEC at these stations can eliminate the contribution of zonally drifting irregularity on TEC gradient variation. However, in case of the single station-method we must note that the background ionospheric plasma drift/circulation speed can potentially inflate as well as deflate the estimated TEC gradient values obtained.

- (d) **If you look at Figures 3b and 3d, the peaks of the red and blue curve matches, but their values say a different story. The value of ROTI-index in Figure 3b is higher than that in Figure 3d. But the values of the spatial gradient show an opposite trend. The value of spatial gradient in Figure 3b is lower than that in Figure 3d. So in terms of ROTI, the ionospheric scintillation is stringer in Figure 3b than 3d. But in terms of spatial gradient, it looks opposite. How to explain it.**

Response:

The values of ROTI in each panel of Figure 3 (a-d), shown as representative cases, was greater than 0.5 TECU/min, a threshold value showing the presence of irregularities. However, they show difference in the strength of irregularities. These difference could be attributed to the difference in the strength of PRE, and other factors. Similarly, the value of the spatial gradient in TEC was different. For example, the value of the spatial gradient in TEC in Figure 3d is higher than that in Figure 3b, while ROTI value in Figure 3b is higher than that in Figure 3d. This might indicate the difference in the cause of the maximum enhancement/reduction in the gradient in TEC and ROTI, for example zonal neutral wind and ExB drift. (Page 12, Figure 3).

- (e) **Figure 3(c): It has almost similar +ve and -ve phases around 16-22 hours. What do the negative phase of the spatial gradient mean physically?**

Response:

When we apply Equation 1, we might obtain positive and/or negative values in the gradient of TEC, mostly around 16-22 hrs. Both the positive and negative phase indicates the gradient in TEC. These values are the relative TEC/plasma density between the two stations. The negative value in gradient of TEC indicates the higher TEC/plasma density over DEBK relative to ASAB, i.e., a reduction in TEC/plasma density over ASAB, showing a decrease in plasma density over ASAB compared to DEBK.

- (f) **The authors here have just shown 4 cases where ionospheric irregularities were present. They also need to show cases when there were no ionospheric irregularities.**

Response:

Thank you for the comment. Cases where absent in the occurrence of ionospheric irregularities were presented in the modified manuscript in Figure 4 (e-h). (Page 14, Figure 4)

- (g) **Figure 4 (a-c): The authors need to modify the color codes of the three figures to make it clear. Right now, the minimum limit of ROTI in Figure 4(a-b) is set at 0.5 which is considered as the onset of ionospheric irregularities. Set it to zero so that a clear picture can be seen.**

Response:

It is a good comment. The color codes of Figure 4 (a-c) given in the manuscript were modified. (Page 16, Figure 6 (left panel))

- (h) **The manuscript do not show any evidence yet, to prove the spatial gradient can be used as an indicator of ionospheric irregularities. It is in a stage where it actually investigates the relationship between spatial gradient of TEC and ionospheric irregularities. So I will suggest the authors suitably change the title of the manuscript. Technical:**

Response:

It is good comment. We presented the relationship between the spatial gradient in TEC and the occurrence

of ionospheric irregularities (Figure 7) as suggested. The spatial gradient of TEC and ROTI correlates with correlation coefficients ($C = 0.58$ for DEBK, $C = 0.53$ for ASAB). This could lead us to relate the spatial gradient of TEC and the occurrence of ionospheric irregularities. Studies indicate that the gradient of TEC can be computed from a pair of closely-spaced receiver stations such that the two receivers share the same GPS satellite (less than 2°). In our case, however, the two stations are separated by 5° . The moderate correlation obtained might be attributed to the wider longitudinal separation (5°) between the two stations. The other factor for the moderate correlation between the gradient of TEC and occurrence of ionospheric irregularities might be the way ROTI was computed (since ROTI contains both the spatial and temporal variation in TEC). If we can reduce the contribution of the temporal part of ROTI, we may get a better relationship. **(Page 1-16; Page 17-18: Figure 7 and 8)**

The title of the manuscript is modified as:

Investigation of the relationship between the spatial gradient of total electron content (TEC) between two nearby stations and the occurrence of ionospheric irregularity

(i) **Page 8: line 3: Figure 2a and d should be Figure 2 (a-d).**

Response:

Thank you. We modified, as suggested.

List of all relevant changes made in the manuscript:

- We modified the title
- We modified the abstract based on the added figures
- We used new terminology, standard deviation of TEC, $\sigma(\Delta TEC/\Delta lon)$, to show the relation between spatial gradient of TEC and occurrence of ionospheric irregularities.
- We reformulated the introduction.
- We rearranged some of the statements in “Data and Analysis Method“ section.
- Figures are added.
- Discussions part of the results are modified

Thank you very much !

References

- Muella, M., De Paula, E., Kantor, I., Batista, I., Sobral, J., Abdu, M., . . . Smorigo, P. (2008). Gps l-band scintillations and ionospheric irregularity zonal drifts inferred at equatorial and low-latitude regions. *Journal of Atmospheric and Solar-Terrestrial Physics*, 70(10), 1261–1272.
- Mungufeni, P., Jurua, E., & Habarulema, J. (2016). Trends of ionospheric irregularities over African low latitude region during quiet geomagnetic conditions. *J. Atmos. Solar Terr. Phys.*, 138-139, 261-267. doi: <http://dx.doi.org/10.1016/j.jastp.2016.01.015>
- Tsunoda, R. (1985). Control of the seasonal and longitudinal occurrence of equatorial scintillations by the longitudinal gradient in integrated E region pederson conductivity. *J. Geophys. Res.*, 90, 447..

Spatial Investigation of the relationship between the spatial gradient of total electron content (TEC) between two nearby stations as indicator of and the occurrence of ionospheric irregularity

Teshome Dugassa^{1,2}, John Bosco Habarulema^{3,4}, and Melessew Nigussie⁵

¹Ethiopian Space Science and Technology Institute, Department of Space Science and Application, Addis Ababa, Ethiopia

²Bule Hora University, College of Natural and Computational Science, Department of Physics, Bule Hora, Ethiopia

³South Africa National Space Agency, Space Science, Hermanus, South Africa

⁴Department of Physics and Electronics, Rhodes University, Grahamstown, South Africa

⁵Washera Geospace and Radar Science Laboratory, Physics Department, Bahir Dar University, Bahir Dar, Ethiopia

Correspondence: Teshome Dugassa (tdugassa2016@gmail.com), John Bosco Habarulema (jhabarulema@sansa.org.za), Melessew Nigussie (melessewnigussie@yahoo.com)

Abstract. The relation between the occurrence of ionospheric ~~irregularity and irregularities~~ and the spatial gradient of total electron content (TEC) ~~derived from two nearby located stations (ASAB:4.34°N, 114.39°E and DEBK: 3.71°N, 109.34°E, geomagnetic), located within the equatorial region, over Ethiopia,~~ during the post-sunset hours ~~over the equatorial region is studied. The ionospheric irregularities could pose serious challenges to satellite-based navigation and positioning applications when trans-ionospheric signals pass through them~~ was investigated. Different instruments and techniques have been applied to study the behavior of ~~these~~ ionospheric irregularities. In this study, the Global ~~positioning system~~ Positioning System (GPS) based derived ~~total electron content (TEC) was used~~ TEC during the year 2014 obtained from the two stations were employed to investigate the ~~spatial relationship between the~~ gradient of TEC ~~between two nearby stations as indicator of occurrence of ionospheric irregularity over the East African sector. The~~ and ionospheric irregularity occurrence. The spatial gradient of TEC ~~between the two stations (ASAB: 4.34° N, 114.39° E and DEBK: 3.71° N, 109.34° E, geomagnetic) located within the equatorial region of Africa were considered~~ ($\Delta TEC / \Delta lon$) and its standard deviation over 15 min $\sigma(\Delta TEC / \Delta lon)$ ~~derived from GPS-TEC were used~~ in this study ~~during the year 2014.~~ The rate of change of TEC ~~based derived index (derived indices (ROTI, ROTI_{ave})) is also used to observe the correlation between the spatial gradient of TEC and the occurrence of ionospheric irregularities. The result obtained shows~~ are also utilized. Our results revealed that most of the maximum ~~positive enhancement/depletions in the spatial gradient of TEC observed in March and September equinoxes are more pronounced between reduction in~~ $\Delta TEC / \Delta lon$ are noticeable during 19:00 LT– 24:00 LT ~~as the large-scale ionospheric irregularities do. Moreover, the observed hours. In some cases, the peak values in the~~ spatial gradient of TEC ~~shows two peaks (in March and September) and they exhibit~~ are also observed during daytime and post-midnight hours. The enhancement in the intensity of $\sigma(\Delta TEC / \Delta lon)$ observed after post-sunset show similar trends with $ROTI_{ave}$, and was stronger/weaker during equinoctial/solstice months. The observed enhancement in the intensity of $\sigma(\Delta TEC / \Delta lon)$ in equinoctial season ~~show an~~ equinoctial asymmetry where the March equinox ~~is was~~ greater than September equinox. The ~~enhancement in the spatial gradient of gradient in~~ TEC and $ROTI_{ave}$ ~~observed~~ during the evening time period also show similar trends ~~but lag~~

~~1-2 hrs from the~~ with equatorial electric field (EEF) ~~.-The~~ but after 1-2 hrs. The relationship between $\sigma(\Delta TEC/\Delta lon)$ and $ROTI_{ave}$ correlate linearly with correlation coefficient of $C = 0.7975$ and $C = 0.7915$ over ASAB and DEBK, respectively. The vast majority of the maximum enhancement/reduction in the spatial gradient of TEC ~~between the two nearby stations could~~ observed during the evening time period may be associated with ionospheric irregularities/equatorial plasma bubbles. In

5 addition to latitudinal gradients, the spatial/longitudinal gradient of TEC has a significant contribution to the computation of TEC fluctuations. The spatial gradient of TEC/electron density near solar-terminator obtained from two nearby located Global Navigation Satellite System (GNSS) receivers may be used as an ~~indicator of the occurrence of ionospheric irregularities~~ alternative method to estimate the strength of the zonal electric field.

10 **Key words:** Spatial gradient of TEC, $ROTI_{ave}$, ionospheric irregularities

1 Introduction

~~The ionosphere is a dispersive medium in which radio signals are refracted depending upon signal frequency and ionospheric~~
The ionosphere, which consists of free electrons and ions, frequently experiences irregular electron density. After sunset, the
ionospheric plasma interchange instabilities present in the equatorial/low-latitude ionosphere generate large-scale depletions in
5 the ambient electron density which leads to the formation of plasma density irregularities that affect radio communication and
navigation system (Basu and Basu, 1981). The generation of the plasma irregularities can be related to the ~~lack of decrease in~~
plasma production immediately after sunset and the fast recombination rate in the E-region ionosphere, which results in a steep
~~gradient in electron density. In the evening hours, the~~ electron density gradient. The large enhancement of F region vertical
plasma drift ~~attest in the evening hours due~~ to the presence of enhanced eastward electric field ~~is also another parameter~~
10 ~~which controls~~ was thought to control the generation of plasma density irregularities (Fejer, 1991; Fejer et al., 2008). This
~~prereversal enhancement in the~~ pre-reversal enhancement (PRE) vertical plasma drift moves the F region to higher altitudes
(Abdu et al., 2009). When the altitude of F-region is high enough to overcome recombination effects, the Rayleigh-Taylor
~~instability mechanisms initiates a~~ (R-T) instability mechanism initiates growth in plasma fluctuations. The R-T instability is
considered primary responsible for the generation of ionospheric plasma density irregularities or plasma bubbles in equatorial
15 and low-latitude region (Rao et al., 2006b; Fejer et al., 1999). Kelley (2009) reported that the existence of equatorial plasma
bubbles (EPBEPBs) is attributed to the instability of the ~~Rayleigh-Taylor (R-T)~~ plasma which is triggered by the intensification
of the eastward equatorial electric field just before its reversal. The ~~R-T instability mechanism is considered the primary~~
~~mechanism responsible for the generation of ionospheric plasma density irregularities or plasma bubbles in equatorial and~~
~~low-latitude region (Rao et al., 2006a; Fejer et al., 1999)~~. A perturbation at the base of the F-region, such as that caused by a
20 ~~gravity wave, can also lead to the growth of the instability, resulting in the formation of plasma bubbles, that is, structures with~~
~~depleted plasma density that produce ESF (Abdu, 2001; Abdu et al., 2009; Kelley, 1989).~~

~~Several studies have indicated that ionospheric irregularities show strong diurnal, seasonal, geographic and solar cycle~~
~~variations (Chu et al., 2005; Kintner et al., 2007). Longitudinal and geomagnetic activity dependency of~~ characteristics of ionospheric
scintillation and ionospheric irregularities over the ~~different equatorial region has also been reported (Burke et al., 2004; Susnik and Forte, 2004)~~
25 ~~Oladipo and Schuler (2013a) studied large-scale ionospheric irregularities at Franceville, Gabon, an equatorial station in the~~
~~African sector for a year (2001/2002) during the last high solar activity. Their results showed the seasonal dependency of~~
~~the occurrence of ionospheric irregularities. Furthermore, the study of Seba and Tsegaye (2015) showed seasonal and annual~~
~~scintillation characteristics over Bahir Dar, Ethiopia. Also, they indicate that the high-level intensity of scintillation occurred~~
~~in March and April, and was low on Solstice days. Tsunoda (1985) proposed that the seasonal and longitudinal occurrences of~~
30 ~~the plasma bubble are most frequent when the solar terminator is most closely aligned with the geomagnetic meridian.~~

~~In the past years, several techniques both from the ground and space-based instruments~~ equatorial and low-latitude region in
different longitudinal sectors during different solar and geomagnetic activities have been studied (e.g., Burke et al., 2004; Paznukhov et al., 2004)
Various instruments such as all-sky imager (Wiens et al., 2006), and very high-frequency radar observation (e.g., Otsuka et al., 2009; Ajith et al., 2009)
been used utilized to study the ~~occurrence behavior~~ of ionospheric irregularities. ~~The widely used instrument was the GPS~~

scintillation index, S4. In the recent years, GNSS (and related scintillations. Recently, Global Navigation Satellite System) based technique has become (GNSS) signal analysis is an important tool for the to study the behavior of ionospheric irregularities (Pi et al., 1997; Nishioka et al., 2008) (e.g., Pi et al., 1997; Nishioka et al., 2008; Watthanasangmechai et al., 2016; Magdaleno et al., 2016) of its growing application in civilian and military applications. Using ground-based GPS measurements over African equatorial and

The inhomogeneity of ionospheric electron distribution can cause sudden, rapid and irregular fluctuations of the amplitude and phase of the received signals, known as ionospheric scintillation (Wernik and Liu, 1974). This inhomogeneity, i.e. spatial plasma density/TEC gradient, is higher at low-latitude regions, region because of geomagnetic storms, equatorial spread F (ESF) and Appleton ionospheric anomaly. As the GNSS signals pass through the ionosphere, the seasonal occurrence of the ionospheric irregularities has been studied by the several workers (Olwendo et al., 2013, 2016; Ngwira et al., 2013; Seba and Tsegaye, 2015). The ionospheric irregularities have adverse effects on irregularities also cause the delay of signals. The classification of the spatial electron density/TEC gradients can be given as latitudinal (north-south) and longitudinal (east-west) (Jakowski et al., 2004). It is normally found in the literature that the spatial plasma density gradients can be represented by means of TEC changes per latitude or longitude (TECU/deg) or by their changes in distance (TECU/km). In addition to causing an integrity threat for life-safety application to air traffic management (Luo et al., 2002; Lee et al., 2011; Rungraengwajai et al., 2015b), the ionospheric TEC gradient is also unfavorable for communication, and surveillance system which depends on trans-ionospheric signals. Therefore, forecasting the probability of occurrence of ionospheric irregularities has become the topic of major research and has drawn the attention of the scientific community. Due to these effects, modeling ionospheric irregularities has been carried out by several researchers (Aarons, 1985; Scherliess and Fejer, 1999; Abdu et al., 2003; Iyer et al., 2006; Mungufeni et al., 2015; Tsegaye et al., 2015). Aarons (1985) developed an analytical equation to yield scintillation excursions based on a series of observations at 254 MHz taken at Huancayo, Peru, as a function of different parameters. Abdu et al. (2003) developed a regional model for the quiet time spread-F distribution in the signal propagation (Foster, 2000). Radicella et al. (2004) and Nava et al. (2007) also presented the contribution of the horizontal gradients of vertical TEC to positioning error. The characteristics of horizontal ionospheric density gradients and their effects on trans-ionospheric radio wave propagation have been studied at different latitudes (Jakowski et al., 2005; Radicella et al., 2004). It has been reported that the majority of large/steep gradient TEC gradients are associated with equatorial plasma bubbles (Pradipta and Doherty, 2016). Rao et al. (2006b) estimated ionospheric spatial gradient from F-region peak electron density (NmF2) data using a chain of radio soundings. Based on the GNSS data acquired by dense distribution of receivers over Brazilian longitude sector. Iyer et al. (2006) developed an empirical model of magnetic quiet time scintillation occurrence at Indian equatorial and low-latitudes. Mungufeni et al. (2015) developed an empirical model for the probability of, Cesaroni et al. (2015) highlights the relationship between intensity and variability of TEC gradients and the occurrence of ionospheric irregularities during geomagnetic quiet conditions over the African equatorial region. Moreover, Taabu et al. (2016) predicts scintillation.

Previous studies attempt to explain the relation between the latitudinal (N-S) gradient of TEC surrounding the anomaly region and ionospheric scintillation over East African region using neural network during the ascending phase of sunspot cycle 24.

different sectors (Mendillo et al., 2001; Valladares et al., 2001; Rao et al., 2006c; Ray et al., 2006; Muella et al., 2008). Mendillo et al. (2001) pointed out that equatorial ionization anomaly (EIA) strength at sunset is the best available precursor for pre-midnight ESF. Using latitudinal distribution of TEC measurements at about 20:00 LT, Valladares et al. (2001) observed a high crest-to-trough ratio prevalent to ESF days. Recently, Seba et al. (2018) investigated the relation between equatorial ionization anomaly and night time ESF over East Africa longitudinal sector using data from ground-based Global Positioning System (GPS) stations and a horizontal meridional neutral wind model. To identify signals which severely suffer from ionospheric gradient, Ravi Chandra et al. (2009) and Rungraengwajjake et al. (2015b) used rate of change of TEC (ROT) and rate of change of TEC index (ROTI). From the definition, however, ROTI mixes both the spatial and temporal gradients of TEC variations. To show the relation between EIA and ESF, Seba et al. (2018) used ROTI and crest-to-trough ratio. Even though, the characteristics of ionospheric irregularities/plasma bubbles over equatorial/low-latitude region of Africa under different solar and geomagnetic activities were discussed (Seba and Tsegaye, 2018), a limited number of studies have been carried out over the region relating the latitudinal/longitudinal gradient of TEC/plasma density and the occurrence of ionospheric irregularities.

~~The evening prereversal enhancement (PRE) The PRE of the vertical plasma drift has important consequences for the Appleton density anomaly and the stability of the nighttime ionosphere. Studies show that the occurrence of ESFs is dependent on an increase with maximum $E \times B$ drift velocity (Whalen, 2001). Using multi-instrument observation, Dabas et al. (2003b) suggested that the equatorial electrojet (EEJ) is a useful parameter for predicting the EPBs development. The PRE in the eastward electric field component near sunset in is one of the most important features of the equatorial ionosphere is a phenomenon that has been well reported and studied (see., Kelley, 2009). Several theories have been proposed to explain the PRE (Rishbeth, 1971a; Farley et al., 1986). Low-latitude/equatorial F-region vertical plasma drifts have been measured extensively using coherent and incoherent scatter radar measurements at the Jicamarca Radio Observatory and they have also been inferred from daytime magnetometer (e.g., Anderson et al., 1986) nighttime ionosonde observations (e.g., Abdu et al., 1981). It has been suggested that the longitudinal which uplift the F-layer and create a conducive condition for irregularity formation under R-T instability mechanism. The causes of the enhanced horizontal electric field have been discussed and modeled in several articles (e.g. Rishbeth, 1971b; Farley et al., 1986b; Eccles, 1998; Kelley et al., 1998). Longitudinal gradient of integrated Pederson conductivity in the E-region at sunset time can play a positive role in strengthening the evening pre-reversal enhancement magnitudes (Tsunoda, 1985; Batista et al., 1986) that exist across sunset terminator affects the strength of PRE and the generation of ionospheric irregularities (Tsunoda, 1985). However, over African longitude sector, it may not be easy to have it is not easy to obtain the longitudinal gradient of electron density as ionosondes over Africa longitude sector as radar, ionograms and/or incoherent scatter measurement are not available in nearby locations and see the correlation between and study the relationship between the electron density gradient and occurrence of irregularities. A closely found GPS receivers may be a good option to ionospheric irregularities. It is generally known that TEC is the integral of electron density, so closely located GPS receivers would help us to examine the strength of the zonal electric field and investigate the relation between longitudinal gradient of total electron content derived from GPS receivers the gradient of TEC and occurrence of~~

ionospheric irregularities. In the present study, we investigate the longitudinal gradient of total electron content derived from two close by GPS stations over Ethiopia (Debark) and Eritrea (Asab) as indicator of irregularity. Investigating the relationship between the spatial gradient of TEC and occurrence of ionospheric irregularities, and discuss the probability of occurrence of ionospheric irregularities irregularity using ground GPS-TEC receiver from two nearby located stations is the aim of the current study. The relation between the daytime eastward equatorial electric field derived from the equatorial electric field (EEF) model and the daytime equatorial electrojet derived from magnetometer measurements will be discussed. (EEJ) obtained from ground based magnetometer measurements were also discussed. The study is the first of its kind in the African sector to present the relation between the spatial gradient of TEC and occurrence of ionospheric irregularities. The gradients of plasma density might be considered as an important parameter in the modeling of ionospheric irregularities and mitigating positioning errors on GNSS based application.

2 Data and analysis method

The present study has been carried out using receiver-independent exchange (RINEX) data from dual frequency GPS receivers located at Debark, Ethiopia and Asab, Eritrea obtained from (The GNSS data used for this study were obtained from University NAVSTAR Consortium (UNAVCO) database (<http://www.unavco.org/>)). We used data from two receiver stations located in the East African region at Debark (Geog. Lat. 13° N, Geog. Long. 37.65° E, Geomag Lat. 4.13° N) and Asab (Geog. Lat. 13° N, Geog. Long. 42.65° E, Geomag. Lat. 4.85° N) for the period 2014. The receiver-independent exchange (RINEX) observation files obtained from the IGS website were processed by the GPS-TEC program application software developed at Boston College (Seemala and Valladares, 2011) was applied to derive TEC values from each dual frequency GPS receiver. The study focuses on the year 2014. The TEC analysis software uses the phase and code values for both L1 and L2 GPS frequencies to eliminate the effect of clock errors and tropospheric water vapor to calculate relative values of slant TEC (Sardón and Zarraoa, 1997; Arikan et al., 2008). In order to avoid the multipath effects, different authors have used observation data of above certain cutoff mask ranging from 15° to 35° (Chu et al., 2005; Mushini and Pokhotelov, 2011). In the current study, we used an elevation cutoff mask of 30° . Average VTEC values are obtained by averaging VTEC over 30 min interval for all satellites in view with elevation angle above 30° . Using the GPS-TEC data collected from these was used for all the VTEC computed. Table 1 gives the list of all the stations for which data has been used in this study.

There are two independent ways of estimating the TEC gradient values using ground based GPS receiver data (e.g., Lee et al., 2007, 2010). The first method uses a pair of closely spaced receiver stations, looking at the same GPS satellite to calculate the difference in TEC values between the two neighboring ionospheric piercing points (IPP) at any given time. The second method uses a single GPS receiver station to infer the spatial TEC gradient values based on the observed temporal rate of change in TEC. In the current study, we have applied the first method to obtain the spatial gradient of TEC. Using the computed VTEC determined from the two receiver stations, the spatial gradient of TEC (the difference of TEC between the two receivers) were two stations per longitudinal separation) was computed for every time and then analyzed to show the possible indicator of F-region ionospheric irregularity occurrence. The spatial gradient of TEC between the two nearby we analyzed its diurnal,

monthly and seasonal variations. The two stations are located nearly along the same geographic latitude with longitudinal separation of about $\sim 5^\circ$ or corresponding spatial separation of 535.7 km. Stations with the same latitude were selected to examine only the contribution of the longitudinal gradient of TEC to the generation of ionospheric irregularities expressed by ROTI. Vertical TEC (VTEC) values obtained by averaging the VTEC over 30 min intervals for a satellite and then averaged over all satellites in view are used in the computation of the gradient of TEC. The spatial gradient of TEC utilized in this study were computed using Eq. (1) (Lee et al., 2007; Ravi Chandra et al., 2009; Cesaroni et al., 2015).

$$\text{Spatial gradient of TEC}(t) = \frac{VTEC_{asab}(t) - VTEC_{debk}(t)}{d} \frac{VTEC_{asab}(t) - VTEC_{debk}(t)}{\Delta lon} = \frac{\Delta TEC}{\Delta lon} \quad (1)$$

where d represents the separation distance Δlon represents the difference in the longitude between the two stations. In this study, we applied standard deviation of the spatial gradient of TEC over 15 min, $\sigma(\Delta TEC/\Delta lon)$, to examine the relation between spatial gradient (zonal or E-W gradients) of TEC and occurrence of ionospheric irregularities.

ΔH -values (ΔH refers to the deviation of the horizontal component of the earth) The time variation of TEC also known as rate of change of TEC (ROT) and its derived indices are a good proxy for the phase fluctuation, which is a measure of large-scale ionospheric irregularities (Aarons et al., 1997) were used in this study. These kinds of indices can be used to characterize all the known features of equatorial spread F (ESF) (Mendillo et al., 2000). The rate of change of TEC (ROT) is given by

$$ROT = \frac{TEC_k^i - TEC_{k-1}^i}{t_k^i - t_{k-1}^i} \quad (2)$$

where i is the visible satellite and k is the time of epoch and ROT is in units of TECU/min. The ROTI is defined as the standard deviation of ROT over a 5-min period and mathematically given by Eq. (3) (Pi et al., 1997; Bhattacharyya et al., 2000; Nishioka et al., 2008). Usually, $ROTI > 0.5$ TECU/min indicates the presence of ionospheric irregularities at scale lengths of a few kilometers (Ma and Maruyama, 2006).

$$ROTI = \sqrt{\langle ROT^2 \rangle - \langle ROT \rangle^2} \quad (3)$$

Oladipo and Schuler (2013b) employed the idea of Mendillo et al. (2000) to obtain a new index called $ROTI_{ave}$ index given in Eq. (4). $ROTI_{ave}$ index is the average of ROTI over 30 min interval for a satellite and then averaged over all satellites in view. The index gives average level of irregularities over half an hour. Recently, $ROTI_{ave}$ has been applied to demonstrate and explain the level of ionospheric irregularities over low-latitude/equatorial region of Africa (Oladipo et al., 2014; Bolaji et al., 2019; Dugassa

In this study, the rate TEC fluctuation index (ROTI) and ($ROTI_{ave}$) (Pi et al., 1997; Oladipo and Schuler, 2013b; Oladipo et al., 2014) were used to observe the occurrence of ionospheric irregularities.

$$ROTI_{ave}(0.5hr) = \frac{1}{N} \sum_{n=1}^N \sum_{i=1}^k \frac{ROTI(n, 0.5hr, i)}{k} \quad (4)$$

where n is the satellite number, $0.5hr$ is half an hour (0, 0.5, 1, ..., 23.5, 24 UT), i is the 5 min section within half an hour ($i = 1, 2, 3, 4, 5, 6$), N is the number of satellites observed within half an hour and k is the number of $ROTI$ values available within half an hour for a particular satellite. According to Oladipo and Schuler (2013b), the value of $ROTI_{ave} < 0.4$, $0.4 < ROTI_{ave} < 0.8$ and $ROTI_{ave} > 0.8$, respectively represents the background fluctuation, existence of phase fluctuation, and severe phase fluctuation activities. These threshold values were used to observe the relation between the occurrence of ionospheric irregularities and the spatial gradient of TEC.

The magnetic data used in this study are obtained from International Real-Time Magnetic Observatory Network (INTERMAGNET) and Africa-Meridian B-field Education and Research (AMBER) installed in Addis Ababa (AAE, 9.0° N, 38.8° E, 0.2° N, geomagnetic) and Adigrat (ETHI, 14.3° N, 39.5° E, 6.0° N, geomagnetic), respectively. It provides one minute values of the northward (X), eastward (Y), vertical (Z) components of the Earth's magnetic field (H from its mean night time level) at Addis Ababa and Adigrat have also been used for this study in computing the, from where the horizontal component (H) is computed using Eq. (5).

$$H = \sqrt{X^2 + Y^2} \quad (5)$$

To avoid different offset values of different magnetometers, the nighttime baseline values in the H component (Eq. 6) are first obtained for each day and subtracted from the corresponding magnetometer data sets to obtain the hourly departure of H denoted ΔH expressed by Eq. (7). The baseline value was defined as the average of the H component night time (23:00 - 02:00 LT) value of the Earth's magnetic field.

$$H_o = \frac{H_{23} + H_{24} + H_{01} + H_{02}}{4} \quad (6)$$

where H_{23} , H_{24} , H_{01} , and H_{02} are respectively the hourly values of H at 23:00, 24:00, 01:00 and 02:00 in local time (LT).

$$\Delta H(t) = H(t) - H_o \quad (7)$$

where t is the time in hours ranging from 01:00 to 24:00 LT. The hourly departure ΔH is then corrected for the non-cyclic variation using (Eq. 8). This correction was proposed previously by Rastogi et al. (2004) who defined non-cyclic variation as a phenomenon in which the value at 01:00 LT is different from that of local midnight (24:00 LT).

$$\Delta c = \frac{\Delta H_{01} - \Delta H_{24}}{23} \quad (8)$$

- 5 The hourly departure of H (ΔH) corrected for the non-cyclic variation corresponding to magnetometer data set gives the solar quiet variation (Sq) values as shown in Eq. (9):

$$Sq(t) = \Delta H(t) + (t - 1) * \Delta c \quad (9)$$

where $t = 1$ to 1440.

- The equatorial electrojet current (EEJ) produces a strong enhancement in the H-component magnetic field measured by magnetometers located within $\pm 5^\circ$ of the magnetic equator. Measurements of this magnetic field perturbation in equatorial magnetometers could provide a direct measure of the daytime equatorial electrojet (EEJ) and have strong relationships with dayside vertical velocity ($E \times B$ drift) (Anderson et al., 2004, 2006; Yizengaw et al., 2012). The equatorial stations respond primarily to the EEJ and also to the ring current and the global quiet time Sq current system. However, ground magnetometers just outside the extent of the EEJ ($\sim 6^\circ - 9^\circ$, off the dip equator) exhibit exact response to the ring and Sq currents, but near-zero response to the EEJ. To obtain the contribution of H-component field to the EEJ current, we subtract the H-component value recorded at the off the equator ($\sim 6^\circ - 9^\circ$ geomagnetic) from H-component value measured at the magnetic equator, using Eq. (10). The subtraction has been made to remove the contribution of the ring current and global Sq dynamo from the H-component. Table 1 gives the list of all the stations for which data has been used in this study

$$\Delta H = \Delta H_{AAE} - \Delta H_{ETHI} \quad (10)$$

- 20 where ΔH_{AAE} and ΔH_{ETHI} , respectively, show the hourly departure of H over Addis Ababa and Adigrat.

- The other data source used in this study ~~was is~~ the Real-time model of the Ionospheric Electric Fields (<http://geomag.org/models/PPEFM/RealtimeEF.html>). ~~We have used this model to observe the relation between the equatorial electric field (EEF) and the spatial gradient of TEC between the two receivers.~~ The Prompt Penetration Electric Field Model (PPEFM) (Manoj and Maus, 2012) is a transfer function model which ~~to~~ models the daily variations coming from the solar wind, which are mapped ~~from in the~~ interplanetary electric field (IEF) data. Eight ~~(8)~~ years IEF data from the ACE satellite, radar data from ~~JULIA~~ Jicamarca Unattended Long-Term studies of the Ionosphere and Atmosphere (JULIA) system, and magnetometer data from the CHAMP satellite ~~was were~~ used to derive the transfer function. Using the real-time data from ACE satellite, the transfer function models the current variations in the equatorial ~~ionospheric electric fields~~ ionosphere. The model takes time

Table 1. Location information and the type of data used in this study.

| Name of stations | Code | Geo. lon | Geo. lat | Geom. lon | Geom. lat | Data |
|-----------------------|------|-------------|-------------|--------------|--------------|--------------|
| Asab, Eritrea | ASAB | 42.65° E | 13° N | 114.34° E | 4.85° N | GPS-TEC |
| Debark, Ethiopia | DEBK | 37.65° E | 13° N | 109.24° E | 4.13° N | GPS-TEC |
| Addis Ababa, Ethiopia | AAE | 38.77° E | 9.04° N | 110.47° E | 0.18° N | Magnetometer |
| Adigrat, Ethiopia | ETHI | 39.46° E | 14.28° N | 111.06° E | 5.80° N | Magnetometer |

and location as input parameters and calculates the best estimates of the equatorial electric field. [The model outputs provide the electric field generated as a result of the convective electric field, quiet time electric field, and both.](#) In the present study, we have used only the background quiet-time electric field [to examine the relation between the equatorial electric field \(EEF\) and the spatial gradient of TEC derived from the two nearby stations.](#)

5 ~~Recently, Nayak et al. (2017) used the~~ [The](#) real-time model of electric field [have been used for different case studies over different sectors](#) to observe the influence of prompt penetration electric field (PPEF) on the [variations of total electron content and the](#) occurrence of ionospheric irregularities ~~during 17 March 2015 geomagnetic storm over Indian and Taiwan longitudes. This~~ [\(Nayak et al., 2017; Dugassa et al., 2019\).](#) However, [this](#) model has not been applied yet to explain the electrodynamic phenomena over African low-latitude region. To use ~~this the PPEF~~ model in this region, we ~~first observed the relation between the daytime of quiet time equatorial electric field (EEF) and~~ [presented its relationship with](#) equatorial electrojet (EEJ), ~~which has a direct relation with $E \times B$ vertical drift. To do this, ground-based magnetometer stations one located at magnetic equator and another one at ($6^\circ - 9^\circ$) off-equator~~ [an indicator of the eastward electric field, during the daytime period over the equatorial region of Africa based on ground-based magnetometer measurements](#) (Rastogi and Klobuchar, 1990; Anderson et al., 2002; Yizengaw et al., 2014) ~~have been used.~~ Over East Africa ~~there were~~ [longitude](#), two magnetometer stations, one at Adigrat ;
10 (ETHI, 14.3° N, 39.5° E, 6.0° N, ~~geomagnetic~~) and the other at Addis Ababa ; (AAE, 9.0° N, 38.8° E, 0.2° N ~~geomagnetic~~), [geomagnetic](#) exist. ETHI and AAE stations belong to ~~African Median and B-Filed Education research, (AMBER) AMBER~~ network (Yizengaw and Moldwin, 2009) and ~~International Magnetic Network (INTERMAGNET)~~ [INTERMAGNET](#), respectively. ~~The difference of the horizontal component (H) of geomagnetic field of these station, ΔH gives the equatorial electrojet contribution which is a proxy to daytime electric field. The connection between the occurrence~~ [It has been reported that the strength of EEJ before sunset has a correlation with the generation](#) of ESF during ~~evening sector preceded by the rapid rise in F-layer and the strength of EEJ before sunset has been presented~~ (Kelley, 2009; Burke et al., 2004). Sreeja et al. (2009) reported ~~observational evidence for the plausible linkage between the EEJ electric field variations with the postsunset~~ [nighttime period preceded by rise in the](#) F-region ~~electrodynamics.~~ Furthermore, Hajra et al. (2012) indicate that the afternoon/evening time variation of eastward electric field as revealed through EEJ seems to play dominant role in dictating postsunset resurgence of
20 ~~EIA and consequent generation of spread-F irregularities. Once the relation between equatorial~~ [\(Dabas et al., 2003a; Uemoto et al., 2010; R](#)

The relation between the EEF obtained from the real-time electric field model and ΔH is determined, and the model is found to be reliable. The equatorial electric field were determined. The EEF derived from the model will be real-time electric field model were used in this study to explain the gradient of TEC and occurrence of irregularities.

We also used rate of change of TEC derived index ($ROTI_{ave}$) to observe the presence of ionospheric irregularities. The time variation of TEC also known as rate of change of TEC (ROT) and its derived indices are a good proxy for the phase fluctuation, which is a measure of large-scale ionospheric irregularities (Aarons et al., 1997). These kinds of indices can be used to characterize all the known features of equatorial spread F (ESF) (Mendillo et al., 2000). The rate of change of TEC (ROT) is given by-

$$ROT = \frac{TEC_k^i - TEC_{k-1}^i}{t_k^i - t_{k-1}^i}$$

where i is the visible satellite and k is the time of epoch and ROT is in units of TECU/min. The ROTI was introduced by Pi et al. (1997) to statistically quantify the ROT measurements. The ROTI is defined as the standard deviation of ROT over a 5-min period. Usually, $ROTI > 0.5$ TECU/min indicates the presence of ionospheric irregularities at scale lengths of a few kilometers (Ma and Maruyama (2006)).

$$ROTI = \sqrt{\langle ROT^2 \rangle - \langle ROT \rangle^2}$$

where ROT can be obtained from Eq. (2). Oladipo and Schuler (2013b) employed the idea of Mendillo et al. (2000) to obtain a new index called $ROTI_{ave}$ index given in Eq. (4). $ROTI_{ave}$ index is the average of ROTI over 30-min interval for a satellite and then average over all satellites in view. The index gives average level of irregularities over half an hour. Recently, Oladipo et al. (2014) used $ROTI_{ave}$ to demonstrate and capture the level of ionospheric irregularity over Nigeria. In this study, influence of equatorial electric field on nighttime variations of the spatial gradient of TEC and the rate-TEC fluctuation index (ROTI) (Pi et al., 1997; Oladipo and Schuler, 2013b; Oladipo et al., 2014) were used to observe the occurrence of irregularities the stations ionospheric irregularities.

$$ROTI_{ave}(0.5hr) = \frac{1}{N} \sum_{n=1}^N \sum_{i=1}^k \frac{ROTI(n, 0.5hr, i)}{k}$$

where n is the satellite number, $0.5hr$ is half an hour (0, 0.5, 1, ..., 23.5, 24 UT), i is the ΔH section within half an hour ($i = \min$ and that of ΔH was 1 min. To make their resolution consistent, 5 min average of ΔH of each of the selected quiet days were computed. In this study, 2, 3, 4, 5, 6), N is the number of satellites observed within half an hour and k is the number of $ROTI$ values available within half an hour for a particular satellite. According to Oladipo and Schuler (2013b), the value of $ROTI_{ave} < 0.4$, $0.4 < ROTI_{ave} < 0.8$ and $ROTI_{ave} > 0.8$, respectively represents the background fluctuation, existence of phase fluctuation, and severe phase fluctuation activities. In the present study, these

threshold values of $ROTI_{ave}$ index were used to statistically observe the occurrence of ionospheric irregularities and compare with the spatial gradient of TEC between the two nearby stations ΔH derived from the H-component of the geomagnetic field of the two stations during quiet days of the year 2012 were used. In this year, we have a large number of magnetometer measurements relative to other years. From each month of year 2012, the five quiet international days (total of 38) obtained from (<http://wdc.kugi.kyoto-u.ac.jp/qddays/index.html>) were selected to show the correlation between ΔH and EEJ. Since the EEJ is a day time phenomenon, only the daytime values of EEJ and ΔH during (07:00 to 17:00 LT) were examined.

3 Results and Discussions

3.1 Relation between the day-time Equatorial Electrojet (EEJ) and Equatorial Electric Field Model (EEFM)

Figure 1a presents typical example of the diurnal variation of equatorial electric field and equatorial electrojet EEJ and EEJ current signature of H-component of geomagnetic field on 26 March 2012 while Fig. 1b shows the correlation between the equatorial electrojet derived from (2012. As can be seen in Figure 1a, during the daytime period (07:00 - 17:00 LT), the ΔH and EEJ show similar trends. The relationship between the strength of daytime EEJ derived from ΔH and equatorial electric field (EEF) derived and EEF obtained from equatorial electric field model in the daytime period (was shown in Figure 1b. To show the reliability of EEF model over East African sector, we presented the relationship between ΔH and EEJ for five (5) international quiet days of each month of year 2012. In the analysis, we considered the daytime (07:00 to - 17:00 LT) for some of selected quiet days of month of value of ΔH and EEJ. As depicted in Figure 1b, during daytime period, the year 2012. The equatorial electric field is a key factor in determining the dynamics and structure of the low latitude ionosphere (Fejer, 2011). For the first time it was detected by the Jicamarca (11.95° S, 76.87° W) incoherent scatter radar (ISR) and the Jicamarca Unattended Long-Term studies of the Ionosphere and Atmosphere (JULIA) system during the period from 1998 to 2008. However, there were no direct continuous electric field observations from ground-based and when available, mostly limited to the daytime. Over African region there is no ground-based measurements of the zonal electric fields. Anderson et al. (2002) used the ΔH correlate positively and linearly with EEJ with correlation coefficient, $C = 0.60$. Manju et al. (2012) obtained an excellent agreement with observations at the Indian and South American sectors. Different techniques have been utilized to estimate the ionospheric electric field (e.g., Hysell and Burcham, 2000; Anderson et al., 2002; Alken et al., Anderson et al. (2002) proposed ΔH deduced from magnetometers and ground-based magnetometers as a proxy of equatorial electrojet current. They reported that the vertical plasma drifts observed by Jicamarca ISR to identify from Jicamarca incoherent scatter radar (ISR) has a positive and linear relationship between the equatorial EEJ and EEJ. Since then, relation with ΔH and henceforth the ΔH is widely known was widely taken as a substitution for the EEJ. To use the ΔH derived from the horizontal (H) component of geomagnetic field over East African sector, AMBER magnetometer data over Adegat, Ethiopia (ETHI) station during the year 2014 were not available. To solve this data gap we used the daytime information of equatorial electric field derived from the real-time prompt penetration electric field model as an option. The relation between the daytime (07:00-17:00 LT) value of ΔH deduced from magnetometers and the Anderson et al. (2006) and Yizengaw et al. (2011) also reported a strong relation between the dayside vertical velocity ($E \times B$ drift) and ΔH . Alken et al. (2013), on the other hand, estimates

the EEJ using CHAMP satellite derived latitudinal current profiles of daytime EEJ along with ΔH measurements from ground magnetometer stations and they showed that any pair of ground magnetometer stations capture the day-to-day strength of the EEJ.

The daytime eastward equatorial electric field obtained from EEFM during the year 2012 were presented in Fig. 1b. As shown in the figure, the daytime equatorial electrojet (ΔH) correlate linearly with quiet-time equatorial electric field model with correlation coefficient of ($R = 0.70$). Studies showed (EEF) in the ionospheric E-region plays an important role in equatorial ionospheric dynamics. It is responsible for driving the EEJ current system, equatorial vertical ion drifts, and the equatorial ionization anomaly. The EEJ is a strong ionospheric current along the magnetic equator driven by the day side eastward electric field. Studies also show that the daytime electrodynamic play a decisive role in the initiation of post-sunset ESF (e.g., Mendillo et al., 2001; Valladares et al., 2001, 2004). Hence, in this study we have used The connection between the occurrence of ESF during the evening sector preceded by the rapid rise in F-layer and the strength of EEJ before sunset has been presented (Dabas et al., 2003a; Burke et al., 2004; Kelley, 2009; Uemoto et al., 2010; Ram et al., 2007). Sreeja et al. (2009) reported observational evidence for the plausible linkage between the daytime EEJ related electric field variations with the postsunset F-region electrodynamic. Furthermore, Hajra et al. (2012) indicate that the afternoon/evening time variation of the eastward electric field as revealed through EEJ seems to play a dominant role in dictating postsunset resurgence of EIA and consequent generation of spread-F irregularities. Since the equatorial electric field derived from EEFM model to show its effect on the post-sunset enhancement of model (EEF) correlate moderately with ΔH over East Africa longitudinal sector, we could use the real-time EEF model over equatorial/low-latitude region of Africa to explain some special features of ionospheric phenomena like plasma density irregularities and the positive/negative in the spatial gradient of TEC and explain the possibility that it could be used as indicator of occurrence of ionospheric irregularities between the two stations.

3.2 Relation between the equatorial electric field (EEF), the spatial gradient of TEC and occurrence of ionospheric irregularities

Figure 2 a and d present examples showing the relation between an enhancement in the spatial gradient of TEC and the equatorial electric field during the pre-midnight period. The red and blue curve indicates the equatorial electric field and the spatial (a-l) shows the diurnal variation of the quiet-monthly mean of spatial gradient of TEC (blue curves) and EEF (along $\sim 40^\circ$ E) (red curves) in the year 2014. We superimpose EEF and spatial gradient in TEC to observe the effect of EEF on the variability of the gradient in TEC and/or occurrence of ionospheric irregularities. In the computation of the spatial gradient of TEC (using Eq. 1), negative/positive values in the gradient of TEC may be observed during the nighttime or daytime. Both the negative and positive differences of TEC between the two stations show the gradient of TEC, respectively. From Fig. 2, it can be observed that the equatorial electric field start rising nearly after 16:00 LT and enhanced in the evening local time at about 18:00 LT. It is obvious that positive/negative gradient in TEC is obtained when the minuend is larger/smaller than the subtrahend. A positive/negative gradient in TEC denotes an enhancement/reduction in TEC or electron density over ASAB relative to DEBK. Gradient in TEC is positive when TEC over ASAB is greater and is negative when TEC over

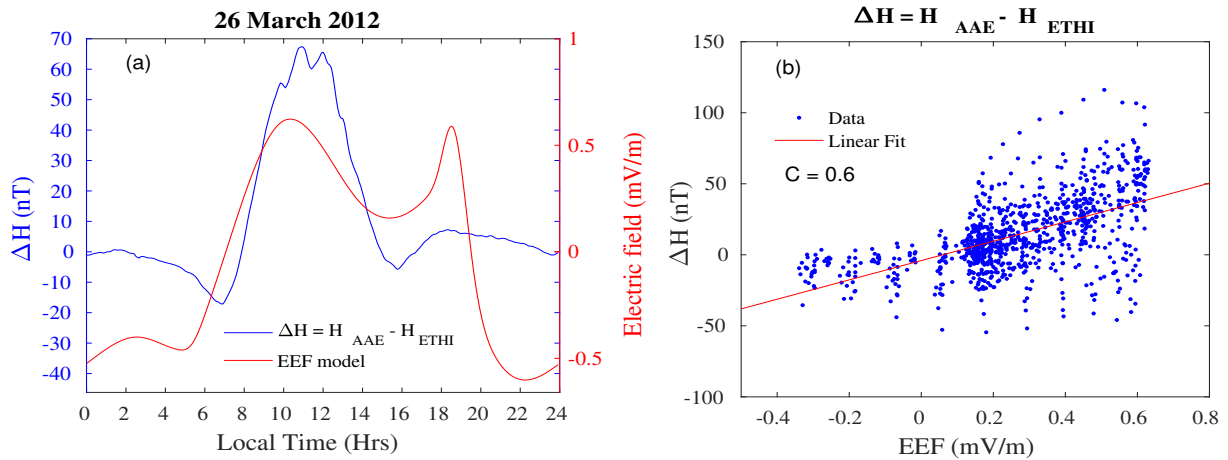


Figure 1. (a) Diurnal-Example showing the diurnal variation of Equatorial Electric field Model-(EEF) Model (red curve) and ΔH (blue curve) during 26 March 2012 and (b) Day-time-The correlation between the equatorial electrojet (EEJ) and quiet-time equatorial electric field model (EEF) during day-time (07:00-17:00 LT) period for quiet days of month-of-year 2012. The red line shows the linear fit of data points.

DEBK is greater. This difference may be attributed to different physical processes, like neutral winds and plasma drift. In this study, the term maximum enhancement/reduction in the gradient of TEC (in terms of magnitude) were used when the nighttime value of gradient of TEC was larger than the daytime value. There were also cases when the gradient in TEC during the daytime was greater than night time values. It can be seen from Figure 2 (red curves) that around evening hours, enhancement in EEF were observed in the equinoctial months and was relatively weak during the June and December solstices. It has been stated that an enhanced eastward electric field will be produced from the electrodynamical interaction of the eastward thermospheric wind with the geomagnetic field around the dip equator at the sunset terminator when longitudinal gradient conductivity exist between the high-conducting day side ionosphere and the low-conducting night side ionosphere (Batista et al., 1986; Heelis et al., 1974). Most of the enhancement of the spatial gradient of TEC was also /reduction in the TEC gradient was observed in the evening local time (18 pre-midnight (19:00 - 24:00)-but lags LT) and postmidnight (24:00 - 06:00 LT) but after 1-2 hours from hr of the post-sunset enhancement of the equatorial electric field. The depletions in the During the nighttime period, the maximum enhancement/reduction in spatial gradient of TEC (not shown here) also shows a similar trend with the equatorial electric field as the maximum positive of found mostly in the range between 5.0 TECU/deg and -5.0 TECU/deg. A variation in the spatial gradient of TEC does. The observed in the pre-midnight may be due to the plasma bubbles (Ratnam et al., 2018). In some days, the spatial gradient of TEC observed during the daytime was relatively small compared to the evening time value for most of the days. The hours. The maximum enhancement/reduction in the gradient of TEC and the peak in the EEF observed during the pre-midnight period was significant during the equinoctial months. After post-sunset period, the maximum enhancement/depletion-reduction in the gradient of TEC in solstice months was small compared to equinoctial months, when PRE electric field observed in the evening period was minimum. Yoshihara et al. (2005) confirm

the larger ionospheric gradients during summer and followed by autumn. The ionospheric gradients are less during winter as compared to summer and autumn. The enhancement/reduction in the gradient of TEC observed in the evening period could be related to the pre-reversal enhancement in PRE in a zonal electric field. Mendillo et al. (2001) have pointed out that the best available precursor for pre-midnight-ESF is the EIA strength at sunset. Using differential TEC profiles, TEC (at 1800 h) – TEC (at 2000 h), Valladares et al. (2004) explained that the pre-reversal enhancement (PRE) of the vertical drift would reenergize the fountain effect.

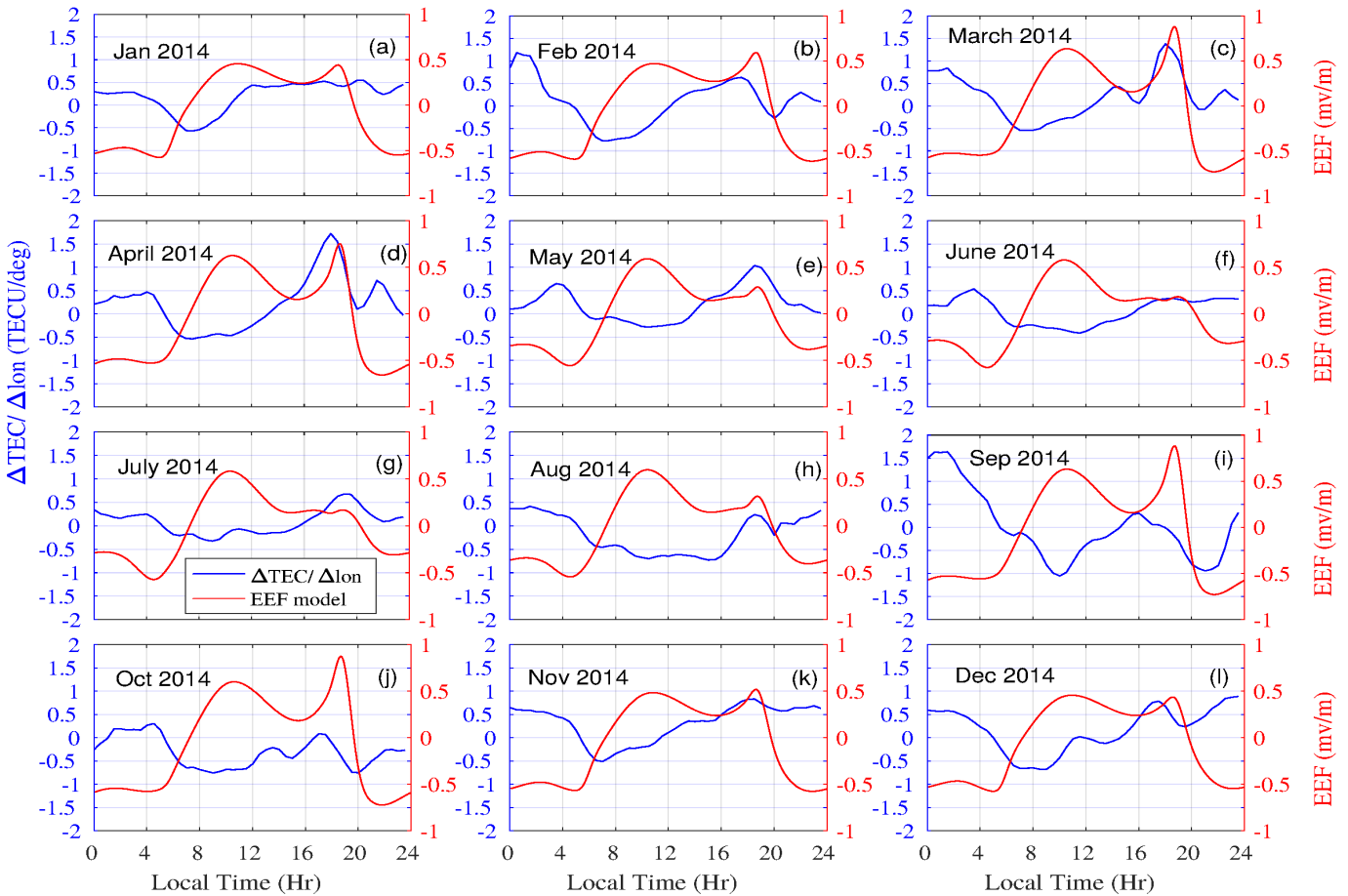


Figure 2. Comparison of Quiet-Monthly Mean of EEF derived from real-time electric field model at about ($\sim 40^\circ$ E) and spatial gradient of TEC between ASAB and DEBK in the year 2014.

Typical examples showing the relation between the spatial gradient of TEC Figures 3 (a - d) shows the diurnal variation of the spatial gradient of TEC (blue curve) and the phase fluctuation index indicated by $ROTI_{ave}$ (red and black curves) over ASAB and DEBK stations. The $ROTI_{ave}$ showing the occurrence of ionospheric irregularities is depicted in Fig. 3a - d. The blue and the red curves, respectively, indicate the spatial values in each panel was greater than 0.4 TECU/min, a threshold value showing

the presence of irregularities in the pre-midnight hours. Likewise, maximum enhancement/reduction in the gradient of TEC between the two GPS stations and the phase fluctuation index ($ROTI_{ave}$) over Asab. In the post-sunset hours, after of TEC were observed during pre-midnight and post-midnight periods. It is evident from Figure 3 during nighttime period (after 18:00 LT, the LT) that the pattern of the two parameters shows a similar trend. The enhancement-ROTI (observed in both stations) and the spatial gradient in TEC show a kind of similar trend. Different researchers used the concept of ionosphere spatial gradient based on multi-GNSS observations within a small scale region to provide corrections and integrity information to the Ground-Based Augmentation System (GBAS) (Rungraengwajjake et al., 2015b; Saito and Yoshihara, 2017). They attribute the large ionosphere spatial gradient to the TEC enhancements and the ionosphere irregularities. Saito and Yoshihara (2017) associated spatial gradient in ionospheric TEC with plasma bubbles. Sun et al. (2013) examined the relationship between the storm-enhanced plasma density (SED)-associated irregularities (ROTI) and TEC gradients over continental United States (CONUS) during the geomagnetic storms. Rungraengwajjake et al. (2015b) analyzed plasma bubbles at postsunset equinox time and observed the higher scales in east-west gradient compared with north-south gradients for GBAS system, however, Cesaroni et al. (2015) reported that north-south gradient in TEC correlates well with ionospheric scintillation than the east-west gradient of TEC. The plasma density variability, either the spatial and/or temporal, causes not only the GNSS-based positioning error but also radio wave scintillation.

The maximum enhancement/reduction in the gradient of TEC and occurrence of irregularities in the associated ionospheric irregularity during the post-sunset period could be explained by the presence of ionospheric electrodynamic. The post-sunset period electrodynamic. It is well known that Earth's equatorial ionosphere presents dynamically temporal and spatial variations. The electrodynamic of low-latitude ionosphere after sunset is influenced by F-region dynamo which is governed by a longitudinal gradient of the electrical conductivity and thermospheric zonal wind (Crain et al., 1993). Anderson et al. (2004) showed that the scintillation activity is related to the maximum $E \times B - E \times B$ drift velocity between 1830 and 1900 LT.

An example of comparison of equatorial electric field model (EEFM) and the spatial gradient of TEC on a) 30 March 2014, b) 10 April 2014, c) 20 September 2014 and b) 10 October 2014. 18:30 LT and 19:00 LT. Mendillo et al. (2001) have pointed out that the best available precursor for pre-midnight equatorial spread F (ESF) is the equatorial ionization anomaly (EIA) strength at sunset, which is in turn influenced by the magnitude of PRE. Using differential TEC profiles, TEC (at 18:00 hr) - TEC (at 20:00 hr), Valladares et al. (2004) explained that the PRE of the vertical drift would re-energize the fountain effect. The postsunset EIA produces a large plasma density gradient from the trough region to the crest region. Takahashi et al. (2016) observed a most steep in TEC gradient with a difference of 30-50 TECU from the inside to outside plasma bubbles.

It has been reported that the eastward component of electric field manifested by the vertical plasma drifts over equator and intensified around/shortly after sunset before reversing to westward is one of the most important parameters responsible for driving many interesting ionospheric phenomena, like the Appleton density anomaly and the stability of the nighttime ionosphere (e.g., Horvath and Essex, 2003; Abadi et al., 2015). In the evening sectors, the vertical drift enhancement is of particular significance as it is the major drivers for the generation of ESF (Farley et al., 1970; Woodman, 1970; Basu et al., 1996;

An example showing relation between the patterns of the spatial gradient of TEC and the $ROTI_{ave}$ on a) 30 March 2014, b) 10 April 2014, c) 20 September 2014 and d) 10 October 2014.

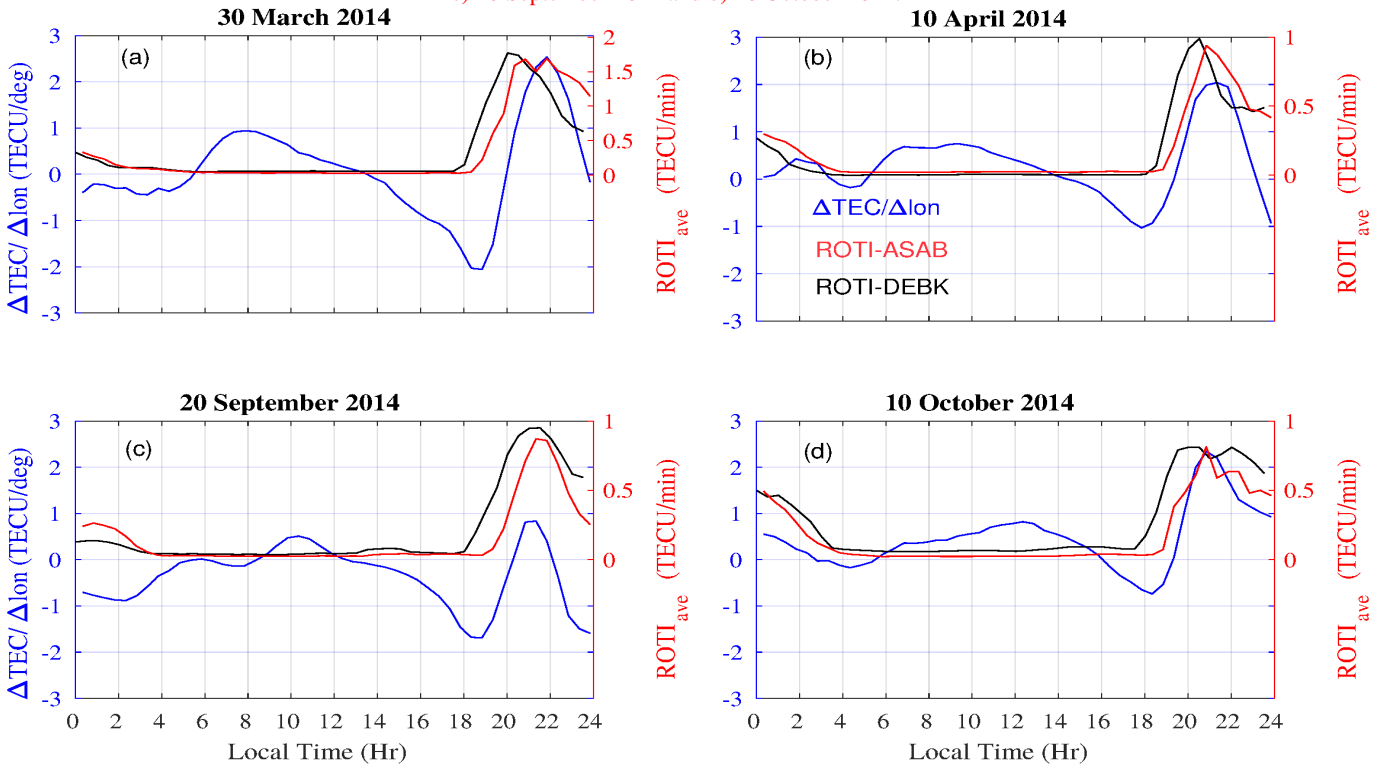


Figure 3. Typical examples of diurnal variation in the spatial gradient of TEC (blue curve) and the ROTI over ASAB (red curve) and DEBK (black curves) on a) 30 March 2014, b) 10 April 2014, c) 20 September 2014 and d) 10 October 2014.

Fejer et al., 1999; Martinis et al., 2005). Tulasi Ram et al. (2006) reported that the rapid enhancement of post-sunset of the zonal electric field leads to a large vertical plasma drift $(E \times B)$, thereby lifting the F-layer to higher altitudes resulting in a condition conducive for the generation of ESF. Vertical drifts are taken as the key parameters determining the dynamics of ionospheric F-region, and the occurrence of ESF. Ionospheric irregularities are mostly observed over equatorial/low-latitude region an hour or two hours after the pre-reversal enhancement (PRE). From the figure, the PRE. Rastogi and Woodman (1978) showed ESF can appear at any time of the night other than the post-sunset period following the abnormal reversal of the vertical F-region drifts to an upward direction, with a delay of about 1-2 hr. As illustrated in Figure 2, the influence of post-sunset enhancement in zonal electric field as shown in the equatorial electric field model has a profound effect on the enhancement of the zonal electric field on the maximum enhancement/reduction in the spatial gradient of TEC during the post-sunset period. This might indicate that can be seen. This could indicate the maximum enhancement/reduction in the spatial gradient of TEC as indicator of and the occurrence of ionospheric irregularities have some degree of relationship.

Figures 4 (a-h) indicate representative cases showing the diurnal variation of $ROTI_{ave}$ over ASAB (red curve) and DEBK (black curve) and $\sigma(\Delta TEC/\Delta lon)$ (blue curve) when the occurrence of ionospheric irregularities. Different researchers used the concept of ionosphere spatial gradient based on multi-GNSS observations within a small-scale region to provide corrections and integrity information to the Ground-Based Augmentation System (GBAS) and they attribute the large ionosphere spatial gradient to the TEC enhancements and irregularity present (left panel) and absent (right panel). It is clearly observed from Figures 4 (a-d) that intensity level of $ROTI_{ave}$ was greater than 0.4 TECU/min indicating the presence of ionospheric irregularities. Figures 4 (e-h), on the other hand, indicate examples when the presence of occurrence of ionospheric irregularities are absent, where the value of $ROTI_{ave}$ was less than 0.4 TECU/min. $ROTI_{ave} > 0.4$ TECU/min indicate the presence of ionospheric irregularities (Oladipo and Schuler, 2013b; Oladipo et al., 2014). As can be seen from Figure 4 (blue curves), the intensity level of $\sigma(\Delta TEC/\Delta lon)$ observed in the evening period was higher when the occurrence of ionospheric irregularity present (Figure 4, left panels) than when the occurrence of irregularity absent (Figure 4, right panels). It is evident from the figures that the strength of $\sigma(\Delta TEC/\Delta lon)$ observed on the nighttime period was greater than the daytime value, as $ROTI_{ave}$ does. The post-sunset plasma bubble irregularities are generated at the bottom side of the F-layer by the sunset enhancement of the zonal electric field called pre-reversal enhancement caused by the the combined action of an eastward thermospheric wind and the longitudinal gradient in ionospheric conductivity that exist along sunset terminator (Rishbeth, 1971b; Fejer et al., 1999). It is well documented that plasma bubble development depends on the linear growth rate for generalized R-T instability process, the flux tube integrated Pedersen conductivity that controls the non-linear development, and density perturbations that are needed to act as a seed to trigger the instability growth. The density gradient control the intensity of the PRE through the E regions electro-dynamical coupling process and the ionosphere irregularities (Rungraengwajiake et al., 2015a; Saito and Yoshihara, 2017). An ionosphere gradient of 518 mm/km was discovered, generated by a plasma bubble (Saito and Yoshihara, 2017) generation of equatorial plasma bubbles (Abdu et al., 2009). Background electron density and its distribution in the ionosphere affects the formation of ionospheric irregularities. The intensity level of $\sigma(\Delta TEC/\Delta lon)$ obtained from two nearby located stations observed near sunset terminator, related with the longitudinal gradient of ionospheric conductivity, could indicate the presence/absence of large-scale ionospheric irregularities. Cesaroni et al. (2015) reported a strong relation between the standard deviation of gradient of TEC and occurrence of ionospheric scintillation.

Figure 5 (a-d) illustrates examples showing the diurnal variation of $\sigma(\Delta TEC/\Delta lon)$ and $ROTI_{ave}$ during some of selected geomagnetic storm days. These storm days are categorized as moderate magnetic storms ($-100 \text{ nT} \leq \text{Dst} \leq -50 \text{ nT}$) (Loewe and Pröls, 1997). When the presence of ionospheric irregularity are observed ($ROTI_{ave} > 0.4$ TECU/min), the magnitude of $\sigma(\Delta TEC/\Delta lon)$ in the post-sunset period show enhancement (for example, 13 September 2014) and when its occurrence suppressed ($ROTI_{ave} < 0.4$ TECU/min), the magnitude of $\sigma(\Delta TEC/\Delta lon)$ reduced (for example, 19 February and 27 August 2014). On these days, the spatial gradient in TEC ($\Delta TEC/\Delta lon$) observed during the daytime hours show maximum enhancement/reduction. The influence of geomagnetic storm on the occurrence irregularities have been studied (e.g., Aarons, 1991; Oladipo and Schuler, 2013a; Kassa et al., 2017). The triggering/inhibition effect of storm on the generation of ionospheric irregularities could be related to the magnitude and direction of z-component of interplanetary magnetic field (Biktash, 2004). The enhancement/reduction in spatial gradient of TEC in the daytime period during geomagnetic storm day appears to show inhibition of ionospheric irregularities. On the other

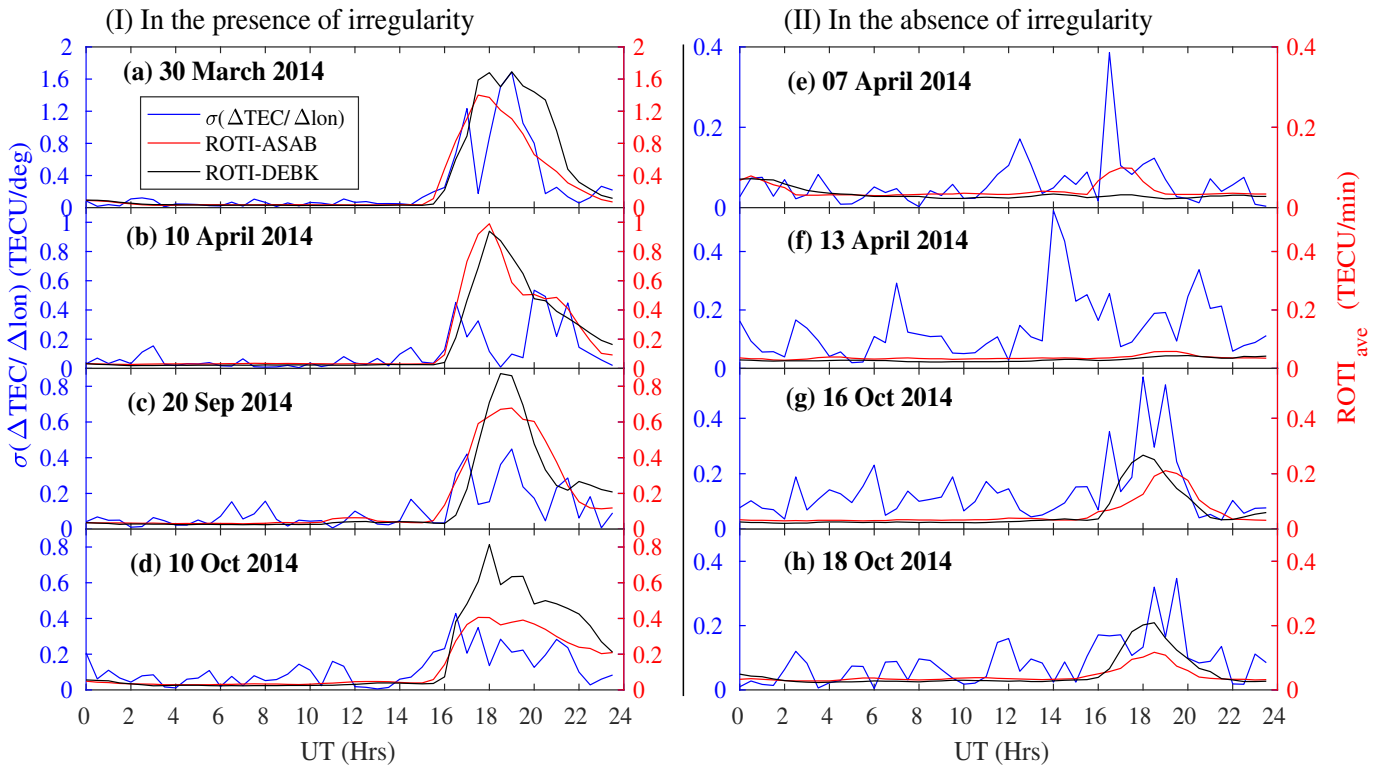


Figure 4. Typical examples showing the diurnal variation of $\sigma(\Delta TEC/\Delta lon)$ (blue curve) and $ROTI_{ave}$ over ASAB (red curve) and DEBK (black curves) (I) in the presence of ionospheric irregularities on (a) 30 March 2014, (b) 10 April 2014, (c) 20 September 2014 and (d) 10 October 2014 (II) in the absence of ionospheric irregularities on (e) 07 April 2014, (f) 13 April 2014, (g) 16 October 2014 and (h) 18 October 2014. Local time (LT) = UT + 3 hr.

hand, the enhancement/reduction in the $\sigma(\Delta TEC/\Delta lon)$ observed during nighttime period indicate the presence/absence of ionospheric irregularity. It is evident from Figures 4 and 5 that the spatial gradient of TEC, $\sigma(\Delta TEC/\Delta lon)$, obtained from two closely located stations could show the presence and absence of ionospheric irregularities.

Figure 4 a and b, Figures 6 (a-d) respectively, show the annual plots of phase fluctuation at Asab and Debarik indicated by variation of $ROTI_{ave}$ index during (over ASAB and DEBK), spatial gradient of TEC ($\Delta TEC/\Delta lon$) and its standard deviation $\sigma(\Delta TEC/\Delta lon)$ in the year 2014. The intensity level of $ROTI_{ave}$ values, $\Delta TEC/\Delta lon$, and $\sigma(\Delta TEC/\Delta lon)$ are indicated in color scale the color bar. As stated by Oladipo and Schuler (2013b), the value of $ROTI_{ave} \geq 0.4$ TECU/min shows the presence of ionospheric irregularity. The occurrence of ionospheric irregularities at the two stations, as indicated by intensity level of $ROTI_{ave}$ value, is a post-sunset phenomenon. The implication of this is that the was predominantly observed in the pre-midnight periods, mainly between 19:00 LT and 24:00 LT. The large-scale ionospheric irregularities, which are responsible for the scintillation of transionospheric-trans-ionospheric signals at GNSS frequencies, are more pronounced during post-sunset hours. The observed phase fluctuation shows monthly variations and there is also a seasonal trend in the

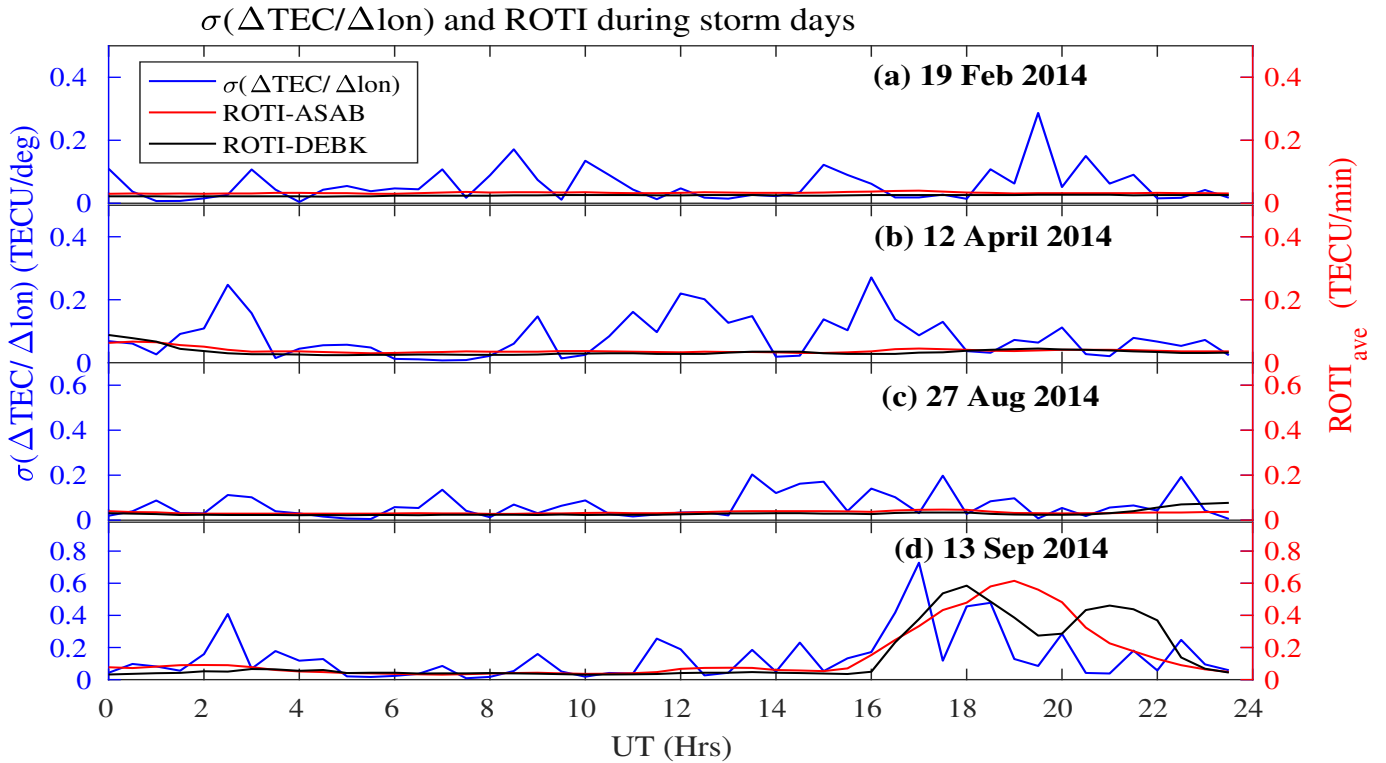


Figure 5. Representative examples showing diurnal variation of $\sigma(\Delta TEC/\Delta lon)$ (blue curves) and $ROTI_{ave}$ over ASAB (red curves) and DEBK (black curves) during geomagnetic storm days (a) 19 February 2014 (b) 12 April 2014 (c) 27 August 2014 and (d) 13 September 2014. Local time (LT) = UT +3 hr.

occurrence of ionospheric irregularity (see., Fig. 9). Maximum irregularities were observed in March equinox months and minimum in June/July. During this period, the occurrence of phase fluctuation showing irregularities is observed mainly between 19:00 LT and 24:00 LT. As stated by Oladipo and Schuler (2013b), the value of $ROTI_{ave} > 0.4$ shows a presence of ionospheric irregularity solstices, respectively.

- 5 Figure 4 c indicates the annual plots of the spatial gradient of TEC between the two nearby GPS stations, Debark (DEBK) and Asab (ASAB) during the year 2014. As already stated in section (2), the two stations are located nearly on the same geographic and geomagnetic latitudes with a longitudinal separation of about 5° or corresponding spatial separation of about 535.7 km. In the computation of the spatial gradient of TEC (Using Eq. 1), negative and positive values of It can be seen from Figure 6c that positive/negative values in the gradient of TEC were observed. From the figure, the maximum positive Gradient in TEC is positive when TEC/negative value of electron density over ASAB is higher, and is negative when TEC/electron density over DEBK is higher. Maximum enhancement/reduction in the gradient of TEC was observed mostly during the post-sunset (18:00 - 24:00 LT) and postmidnight post-midnight (24:00 - 06:00 LT) period. Equation (1) was applied to all days of the (364 days) of year 2014 in computing the spatial gradient of TEC. Out of total of the total observed daily maximum value
- 10

of the gradient of TEC, about 194 days (in percent about 53%) of them fall in this time period intervals. There was also a case where the maximum positive and depletions enhancement/reduction in the value of the gradient of TEC were observed in the early morning period.

5 a) Diurnal variation of the spatial gradient of TEC over ASAB and DEBK, b) Daily maximum value of the spatial gradient of TEC variation, c) Diurnal variation of $ROTI_{ave}$ over ASAB station and d) Daily maximum value variation of $ROTI_{ave}$ over ASAB station in the year 2014

10 The positive enhancement in the gradient of TEC observed during post-sunset and postmidnight showing In Figure 6d the diurnal, monthly and seasonal variations are the other features noticed from Fig. 4 c. The values of the variation in the standard deviation of spatial gradient of TEC observed on equinoctial months was greater than Solstice months. Equinoctial asymmetry in the occurrence of TEC gradient was also observed, where March equinox is greater than September equinox. Similarly, the depletions of the spatial gradient of TEC are mostly observed during post-sunset and post-midnight periods as the maximum positive TEC gradient. The depletions of the gradient of TEC observed during the year 2014 also shows equinoctial asymmetry where the March equinoxes were greater than September equinoxes (not shown) $\sigma(\Delta TEC/\Delta lon)$, was clearly observed and its variation show similarity with variation of $ROTI_{ave}$. Maximum enhancement in $\sigma(\Delta TEC/\Delta lon)$ was observed in the evening time period, 19:00 - 24:00 LT. The seasonal variation in $\sigma(\Delta TEC/\Delta lon)$ also appears frequently in equinoctial months, but rarely in solstice months. Such kind of occurrence variation could be related to the magnitude of $E \times B$ drift. Cesaroni et al. (2015) also found seasonal variation of the TEC spatial gradients and they reported that it is larger during the equinoctial seasons than in the solstice seasons.

Figure 4 d and e present

20 Figures 6 (e-h) respectively, show the daily maximum phase fluctuation index, values of $ROTI_{ave}$ over Asab and Debarik stations, respectively and Fig. 4 f shows the daily maximum of the (over ASAB and DEBK), spatial gradient of TEC ($\Delta TEC/\Delta lon$) and standard deviation of spatial gradient of TEC during $\sigma(\Delta TEC/\Delta lon)$, respectively, in the year 2014. It is clearly observed from the figures that the enhancement in As can be observed from Figures 6 (right panel), the daily maximum value of $ROTI_{ave}$ and gradient of TEC, $\Delta TEC/\Delta lon$ and $\sigma(\Delta TEC/\Delta lon)$ shows monthly and seasonal variations, and the equinoctial asymmetry was an equinoctial asymmetry is also observed. To identify whether the spatial gradient of the total electron content (TEC) between the two nearby stations indicate the occurrence probability of ionospheric irregularity, the rate of change of TEC derived index ($ROTI_{ave}$) described in section (2) expressed by Equation (4) and the spatial gradient of TEC between the two receivers were compared. The daily maximum value of the spatial gradient of TEC between the two stations $\Delta TEC/\Delta lon$ and $\sigma(\Delta TEC/\Delta lon)$ shows similar trends with the daily maximum value of $ROTI_{ave}$ observed over ASAB and DEBK stations. The trend they show has similarity with the time of occurrence of maximum enhancement/reduction, monthly and seasonal variations. Moreover, the seasonal variation observed in both variables exhibits equinoctial asymmetry, where the March equinox was greater than September equinoxes. The mechanism of generation of the enhancement in vertical drift just after sunset was detailed by Farley et al. (1986b). The magnitude of peak vertical drift is known to control the seasonal and day-to-day variations in the occurrence of equatorial spread F (Manju et al., 2009; Tulasi Ram et al., 2006).

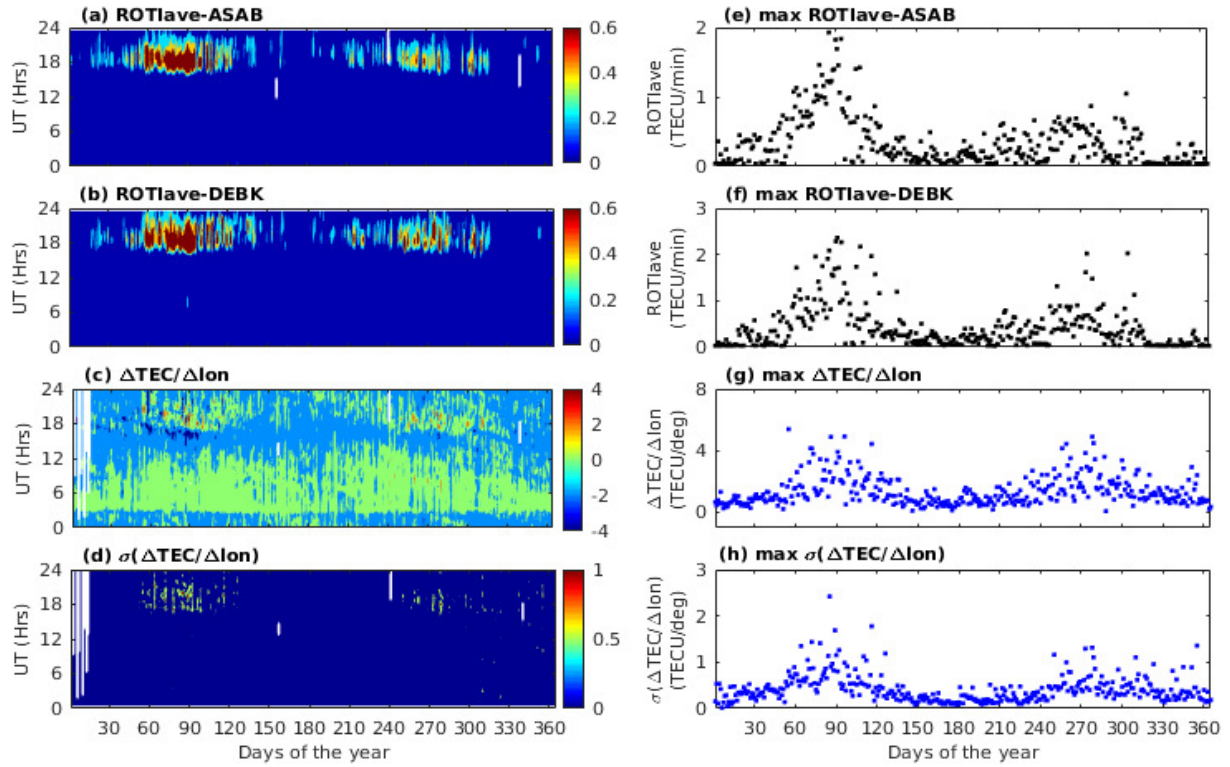


Figure 6. Annual and daily maximum value variation of (a,b) $ROTI_{ave}$ over Asab (ASAB), (c,d) $ROTI_{ave}$ over Debarak (DEBK), (e,f) spatial gradient of TEC ($\Delta TEC/\Delta lon$), (g,h) standard deviation of gradient of TEC $\sigma(\Delta TEC/\Delta lon)$ in year 2014. The $ROTI_{ave}$ in TECU/min and $\Delta TEC/\Delta lon$ in TECU/deg is indicated in color bar. Local time (LT) = UT + 3 hr.

Figure 7 depicts the quiet-monthly mean of $ROTI_{ave}$ (over ASAB and DEBK) (red and black curves) and $\sigma(\Delta TEC/\Delta lon)$ (blue curve) in the year 2014. The enhancement/reduction in the intensity of $\sigma(\Delta TEC/\Delta lon)$ show similar trends with $ROTI_{ave}$, and was stronger/weaker during equinoctial/solstice months. Equinoctial asymmetry both in $ROTI_{ave}$ and $\sigma(\Delta TEC/\Delta lon)$ was also evident from Figure 7, where March equinoxes was stronger than September equinoxes. As expected, the TEC spatial gradients are also found to be larger during the equinoctial seasons than in the solstice seasons.

Figure 8 shows relationship between the standard deviation of spatial gradient of TEC $\sigma(\Delta TEC/\Delta lon)$ and $ROTI_{ave}$ (over ASAB and DEBK) in the year 2014. The daily maximum values of $\sigma(\Delta TEC/\Delta lon)$ and $ROTI_{ave}$ were considered to examine their correlation. The correlation coefficient between $\sigma(\Delta TEC/\Delta lon)$ and $ROTI_{ave}$ is about 0.7915 (in ASAB) and 0.7975 (in DEBK), respectively. Studies indicate that the gradient of TEC can be computed from a pair of closely-spaced receiver stations ($< 2^\circ$) such that the two receivers share the same GPS satellite. In our case, however, the two stations are separated by 5° . The moderate correlation obtained might be attributed to the wider longitudinal separation (5°) between the two stations. The other factor for the moderate correlation between the gradient of TEC and occurrence of ionospheric irregularities might be the way ROTI was computed (since ROTI contains both the spatial and temporal variation in TEC). It is

Seasonal variation of $\sigma(\Delta TEC/\Delta lon)$ and ROTI Year 2014

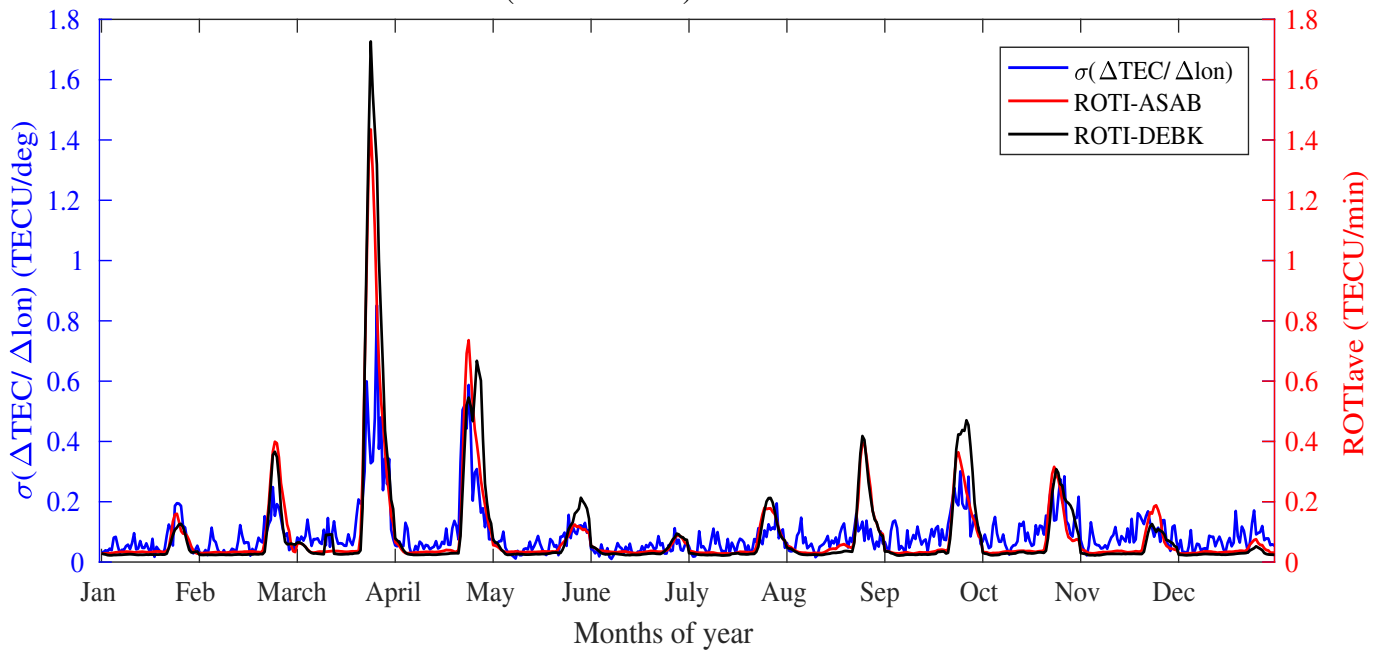


Figure 7. Seasonal variation of $ROTI_{ave}$ over ASAB (red curve), $ROTI_{ave}$ over DEBK (black curve), and $\sigma(\Delta TEC/\Delta lon)$ (blue curve) in the year 2014

well known that ROT is the combination of the spatial and temporal gradients. However, by giving less attention to the spatial gradient effect, previous authors often use $\Delta TEC/\Delta t$ to examine the fluctuation in TEC. It is not only the temporal variation of TEC that contribute to the fluctuation in the phase and amplitude of the signals but also the spatial gradient of TEC. The computed correlation coefficient between the TEC gradient and ROTI, here, gives an indication of the contribution of the spatial gradient of TEC to ROTI (or ROT) usage. This can give the case where the spatial gradient of TEC between two nearby located stations can be used as an indicator of occurrence of ionospheric irregularities. Every night time enhancement/reduction in the gradient of TEC may not be a guarantee to indicate the occurrence/non-occurrence of ionospheric irregularities. However, there are cases which show the occurrence of irregularities over both stations (ASAB and DEBK) when the night time enhancement/reduction in the TEC gradient were observed. Hua and Chunbo (2009) discussed the relation between ROTI index, ionospheric TEC gradient and vertical TEC. Cesaroni et al. (2015) also described the importance of the information provided by the TEC gradients variability and the role of the meridional TEC gradients in driving scintillation. By comparing the zonal and the meridional components of average and standard deviation of ΔTEC , Cesaroni et al. (2015) reported that the North-South (N-S) gradients of TEC are significantly larger than their East-West (E-W) counterparts, regardless of the season. Saito and Yoshihara (2017) associated extreme ionospheric total electron gradient with plasma bubbles for GNSS Ground-Based Augmentation System and they obtained a largest ionospheric gradient of about 3.38 TECU/km. It is suggested that when scintillation events are investigated ionospheric TEC gradient is also one of considerable parameters.

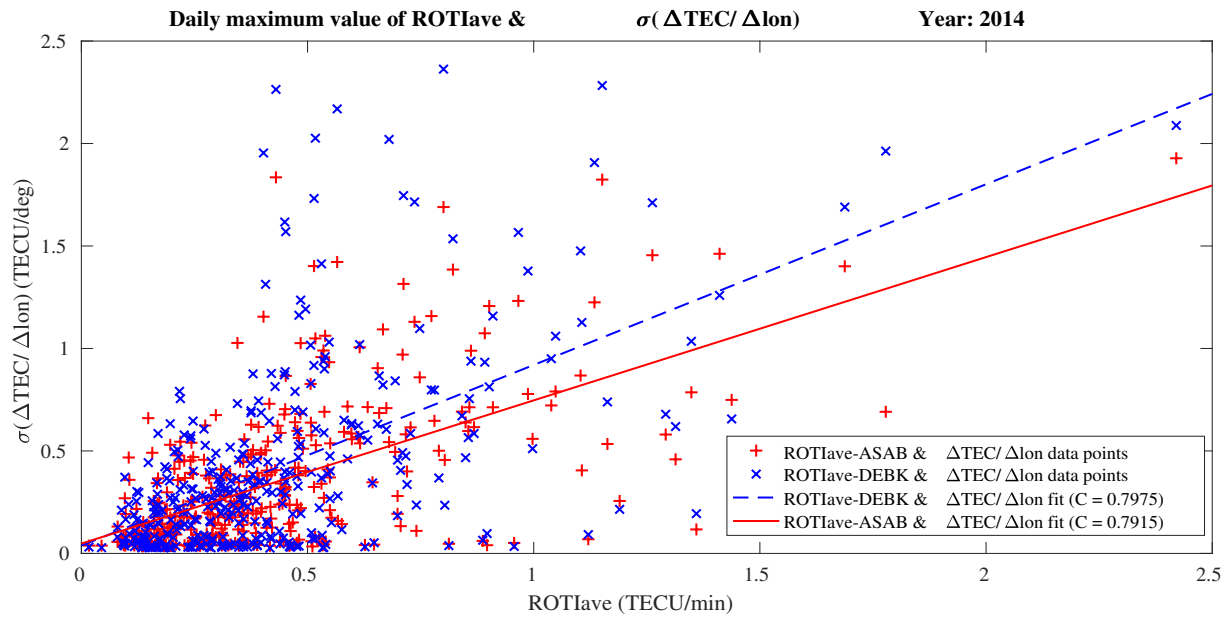


Figure 8. Relation between the daily maximum value of $\sigma(\Delta\text{TEC}/\Delta\text{lon})$ and the daily maximum value of ROTI_{ave} over ASAB (red, +) and DEBK (blue, x) in the year 2014. The blue broken and solid red lines indicate the linear fit between the daily maximum value of $\sigma(\Delta\text{TEC}/\Delta\text{lon})$ and ROTI_{ave} for ASAB and DEBK, respectively.

Figure 9 presents the percentage occurrence of ionospheric irregularities over ASAB (blue) and DEBK (red) in the year 2014. The observation of the percentage occurrence was made for all days of the year 2014 including both quiet and disturbed days. The percentage occurrence of irregularities was calculated by counting the number of days in a month with $\text{ROTI}_{\text{ave}} \geq 0.4$ TECU/min and dividing by the number of days in a month for which the data are available, and multiplied by 100 % .The

two (Oladipo et al., 2014). Since the two stations are close to each other, the occurrence of ionospheric irregularities observed over both stations does not show major differences. Two peaks of irregularity seasons occur occurrence were observed around the middle of the equinoxes (i.e., in March and September) were observed at this station. Previous studies indicated that the seasonal and day-to-day variations in the occurrences of EPB depend on the geographical longitude and latitude. The maximum occurrence of EPB was observed during the equinoxes at longitudes where at both stations. This could be related to the

alignment of the magnetic field lines aligned with a geographic meridian (Burke et al., 2004; Tsunoda, 2005, 2010) (Burke et al., 2004; Tsunoda, 2005, 2010). The seasonal variation of ionospheric irregularities exhibit exhibits an equinoctial asymmetry in its occurrence especially at the two peaks (i.e., in March and September), where March equinox is greater than that of was greater than September equinox. The maximum ROTI_{ave} observed over this station in the year 2014 was about 1.8 TECU/min in March 2014 and minimum level of ROTI_{ave} was observed on December Solstice.

Based on a few station observations, earlier studies indicated that the equinoctial asymmetry in the occurrence of L-band scintillations may be and they attributed to differences in the meridional winds during two equinoxes (e.g., Nishioka et al., 2008; Maruyama et al., 2009).

Nishioka et al. (2008) have ~~shown~~ analyzed the occurrence characteristics of plasma bubbles using ~~GPS-TEC~~ GPS-TEC obtained all over the globe and found equinoctial asymmetry in ~~the occurrence of plasma bubbles in the Asian region~~ its occurrence. They have suggested that equinoctial asymmetry could be due to ~~the~~ the asymmetric distribution of integrated conductivities during these ~~equinoctial~~ periods. Using three ~~ionosondes observations~~ ionosonde observations, Maruyama et al. (2009) reported that meridional wind is the key factor for the equinoctial asymmetry. Using multi-instrument observations, Sripathi et al. (2011) examined the equinoctial asymmetry in scintillation occurrence in the Indian sector and ~~proposed~~ they suggested that the asymmetry in the electron density distribution and meridional winds as a possible causative mechanism. ~~Manju (2013)~~ Manju et al. (2012) also reported equinoctial asymmetry in ESF occurrence and they discussed the possible role of asymmetric meridional winds. ~~Dasgupta et al. (1983) studied the equinoctial asymmetry in equatorial and low latitude F-region ionization distribution and attributed it to neutral composition changes.~~ Manju and Haridas (2015a) observed Manju and Haridas (2015b) observed a significant asymmetry in the threshold height between the vernal equinox and autumn equinox and underlines the distinct differences in the role of ~~neutral~~ neural dynamics in ESF triggering during the two equinoxes. Based on scintillation index (S_4) and GPS-TEC derived indices, the seasonal and equinoctial asymmetry in the occurrence of ionospheric irregularities over equatorial/low-latitude region of African were presented (Susnik and Forte, 2011; Paznukhov et al. (2012)) By employing the horizontal wind model (HWM14), Seba et al. (2018) recently reported that the difference in the wind pattern between March and September is one of the factors for the equinoctial asymmetry. The local time and seasonal trends of occurrence of ionospheric irregularities observed in this study are similar to those reported in the previous studies (~~Aarons, 1993; Basu et al.; Olwendo et al., 2013; Amabayo et al., 2014; Seba and Tsegaye, 2015).~~ The occurrence of equatorial F-region irregularity has been studied, and the frequency of occurrence of equatorial spread F has been found to be higher during solar maximum (Abdu et al., 1998; Mendillo et al., 2000). Similarly, Susnik and Forte (2011); Paznukhov et al. (2012); Oladipo and Oluwalana (2015) studied the seasonal and equinoctial asymmetry (Aarons, 1993; Basu et al., 1988; Olwendo et al., 2013; Amabayo et al., 2014; Seba and Tsegaye, 2015). The equinoctial asymmetries in the occurrence of ionospheric irregularities over African low-latitude sector based on scintillation index (S_4) and GPS-TEC derived index. The maximum $ROTI_{ave}$ observed over this station in the year 2014 was about 1.8 TECU/min in March 2014. It is evident from Fig. 9 that the minimum level of $ROTI_{ave}$ was observed on December 2014. Solstices observed in our case might also be due to the direction of the meridional winds during equinoxes over the stations.

In terms of ~~local time~~ diurnal, monthly, and seasonal behavior the enhancement/reduction in the spatial gradient of TEC and the occurrence of ionospheric irregularities appears to show similar trends. And, it is evident from the above result that the spatial gradient of TEC between two nearby located stations where the two receivers lie nearly along the same latitudes ~~could be used as an indicator of the occurrence of~~ covey insight into the relation between large-scale ionospheric irregularities ionospheric irregularity occurrence. The spatial gradient of electron density (TEC) near solar-terminator obtained from two nearby located GNSS receivers method may be an alternative method to estimate the strength of the zonal electric field. In the current study, the ~~minimum~~ optimum distance between the two ~~stations~~ GNSS receivers and the threshold value of the gradient of TEC that could indicate the ~~probability of~~ occurrence of ionospheric irregularities has not been ~~seen and needs further investigation~~ considered. This will be considered in our future work.

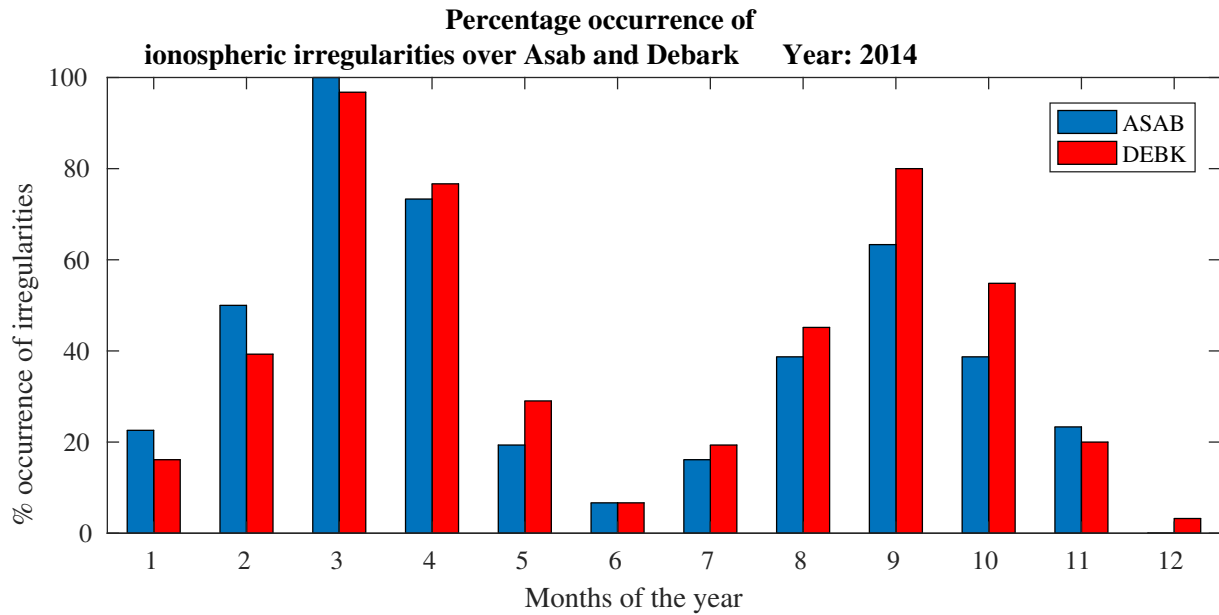


Figure 9. Percentage of occurrence of ionospheric irregularities over ASAB station during (red) and DEBK (blue) stations in the year 2014 based on $ROTI_{ave}$ index.

4 Conclusions

In this study, we present ~~the possibility that for the first time the relationship between~~ the spatial gradient of TEC between two nearby ~~located~~ stations (ASAB and DEBK) ~~over East African sector could be used as indicator of and~~ the occurrence of ~~large-scale ionospheric irregularities~~ ionospheric irregularities over Ethiopia, an equatorial region, using ground based GPS-TEC observations. The following ~~features were observed from the study~~ observations are the summery of our analysis. The daytime equatorial electrojet (EEJ) derived from H-component of geomagnetic field and the real-time electric field (EEF) model (Manoj and Maus, 2012) correlates linearly and positively with correlation coefficient of $C = 0.6$. Most of the ~~daily maximum positive peak enhancement/negative value of reduction value of~~ $\Delta TEC / \Delta lon$ and $\sigma(\Delta TEC / \Delta lon)$ was observed about 1-2 hrs later from post-sunset enhancement of equatorial electric field (EEF), which indicates that EEF and the spatial gradient of TEC ~~was observed in the pre-midnight and post-midnight period~~ has strong relationship. In terms of seasons, ~~months and local times, the maximum positive and months, the nighttime pattern~~ of the spatial gradient of TEC ($\Delta TEC / \Delta lon$) and its standard deviation $\sigma(\Delta TEC / \Delta lon)$ show similar trend with $ROTI_{ave}$. The relation between the standard deviation of the spatial gradient of TEC, $\sigma(\Delta TEC / \Delta lon)$, and ionospheric irregularity occurrence indicated by $ROTI_{ave}$ are presented. The correlation coefficient between $\sigma(\Delta TEC / \Delta lon)$ and $ROTI_{ave}$ show similar trends. Both of them show enhancement during the months of March and September equinoxes. Seasonal $ROTI_{ave}$ was about 0.7975 (in ASAB station) and 0.7915 (in DEBK station). Both $\sigma(\Delta TEC / \Delta lon)$ and $ROTI_{ave}$ show maximum enhancement/reduction during equinoctial/solstice months. Equinoctial asymmetry was also observed in both parameters $\sigma(\Delta TEC / \Delta lon)$ and $ROTI_{ave}$.

where March equinox was greater than September equinox. ~~Peak values in the spatial gradient of TEC and $ROTI_{ave}$ was observed about 1-2 hrs later from post-sunset enhancement of equatorial electric field (EEF). There is also a case where the depletions of the gradient of TEC shows similar trends as the positive maximum value of the TEC gradient~~The intensity level of $\sigma(\Delta TEC/\Delta lon)$ was stronger/weaker when the occurrence of ionospheric irregularity is present/absent. When the occurrence
5 of ionospheric irregularities are suppressed (for example, during geomagnetic disturbed conditions), the nighttime peak value of $\sigma(\Delta TEC/\Delta lon)$ was smaller. Based on the above results, the strength of spatial gradient of TEC between the two nearby ~~stations which lies located stations lying~~ along the same ~~geographic and~~ geomagnetic latitudes could ~~be used as an indicator of the occurrence~~ indicate the presence of large-scale ionospheric irregularities. ~~In this study, we have also used the equatorial electric field model to relate the~~ The spatial gradient of TEC ~~with the phase fluctuation index ($ROTI_{ave}$)/electron density~~
10 near-solar terminator obtained from two nearby located GNSS receivers method may be an alternative method to estimate the strength of the zonal electric field. The threshold value of the gradient of TEC and ~~the minimum separation distance between stations were not presented~~ its standard deviation $\sigma(\Delta TEC/\Delta lon)$ and the minimum longitudinal separation between two stations that could led us to predict the occurrence of ionospheric irregularities are not addressed in the current study and this will be considered in the future investigation.

15 Acknowledgments

~~The Authors~~ We thank Ethiopian Space Science and Technology Institute (ESSTI) for facilitating conditions to do this research. We also acknowledge the administration and staff the Space Science Directorate of the South African National Space Agency (SANSA) for the support during the research visit of the first author to the institution. The authors would like to express their gratitude to the International GNSS Service (IGS) for providing the GPS data ~~and downloaded from the website: (ftp://cddis.gsfc.nasa.gov.~~ We acknowledge for providing the data the Prompt penetration equatorial electric field model. ~~We also~~). We thank the ~~AMBER and INTERMAGNET magnetometer data centers for~~ Cooperative Institute for Research in Environmental Sciences (CIRES) team for real-time PPEEFM model at <http://geomag.org/model/PPEEFM/RealtimeEF.html>. We are also grateful to the online AMBER (<http://magnetometers.bc.edu/index.php/>) and INTERMAGNET (<http://www.intermagnet.org/>) for freely providing magnetometer data. Melessew Nigussie work has been supported by Air
25 Force Office of Scientific Research, Air Force Material Command USAF under Award No.FA9550-16-1-0070. T. Dugassa, thanks Bule Hora University for permitting study leave.

Data availability

The data used in this study were obtained from <ftp://cddis.gsfc.nasa.gov>, <http://geomag.org/models/PPEEFM/RealtimeEF.html>, <http://magnetometers.bc.edu/index.php/>, <http://www.intermagnet.org/>, and http://isgi.unistra.fr/data_download.php.

Competing interests

The authors declare that they have no conflict of interest.

References

- Aarons, J.: Construction of a model of equatorial scintillation intensity., *Radio Sci.*, 20(3), 397-402, <https://doi.org/http://dx.doi.org/10.5194/angeo-32-7-2014>, 1985.
- Aarons, J.: The role of the ring current in the generation or inhibition of equatorial F layer irregularities during magnetic storms, *Radio Science*, 26, 1131–1149, 1991.
- Aarons, J.: The longitudinal morphology of equatorial F layer irregularities relevant to their occurrence., *Space Sci. Rev.*, 63, 209., 1993.
- Aarons, J., Mendillo, M., and Yantosca, R. G.: GPS phase fluctuations in the equatorial region during sunspot minimum., *Radio Sci.*, 32, 1535-1550., 1997.
- Abadi, P., Otsuka, Y., and Tsugawa, T.: Effects of pre-reversal enhancement of $E \times B$ drift on the latitudinal extension of plasma bubble in Southeast Asia, *Earth, Planets and Space*, 67, 74, 2015.
- Abdu, M.: Outstanding problems in the equatorial ionosphere-thermosphere electrodynamics relevant to spread F., *J. Atmos. Solar-Terr. Phys.*, 63, 869-884, 2001.
- Abdu, M. A., Bittencourt, J. A., and Batista, I. S.: Magnetic declination control of the equatorial F region dynamo field development and spread F., *J. Geophys Res. (USA)*, 86, 11443, 1981.
- 15 Abdu, M. A., Batista, I. S., Rios, V. H., and Medina, C.: Equatorial spread F occurrence statistics in the American longitudes: Diurnal, seasonal and solar cycle variations., *Adv. Space Res.*, 22(6), 851-854, 1998.
- Abdu, M. A., Batista, I. S., Takahashi, H., MacDougall, J., Sobral, J. H., Medeiros, A. F., and Trivedi, N. B.: Magnetospheric disturbance induced equatorial plasma bubble development and dynamics: A case study in Brazilian sector., *J. Atmos. Solar-Terr. Phys.*, 108(A12), 1449, <https://doi.org/10.1029/2002JA009721>, 2003.
- 20 Abdu, M. A., Batista, I. S., Reinisch, B. W., de Souza, J. R., Sobral, J. H. A., Pedersen, T. R., Medeiros, A. F., Schuch, N. J., and de Paula, E. R., a G. K. M.: Conjugate Point Equatorial Experiment (COPEX) campaign in Brazil: Electrodynamic highlights on spread development conditions and day to day variability, *J. Geophys. Res.*, 114, A04308, <https://doi.org/10.1029/2008JA013749>, 2009.
- Ajith, K., Tulasi Ram, S., Yamamoto, M., Otsuka, Y., and Niranjana, K.: On the fresh development of equatorial plasma bubbles around the midnight hours of June solstice, *Journal of Geophysical Research: Space Physics*, 121, 9051–9062, 2016.
- 25 Alken, P., Chulliat, A., and Maus, S.: Longitudinal and seasonal structure of the ionospheric equatorial electric field, *Journal of Geophysical Research: Space Physics*, 118, 1298–1305, 2013.
- Amabayo, E., Jurua, E., Cilliers, P., and Habarulema, J.: Climatology of ionospheric scintillations and TEC trend over the Ugandan region. , *Adv. Space Res.*, 53,734-743., 2014.
- Anderson, D., Anghel, A., Yumoto, K., Ishitsuka, M., and Kudeki, E.: Estimating daytime vertical $E \times B$ drift velocities in the equatorial F-region using ground-based magnetometer observations, *Geophys. Res. Lett.*, 29(12), 1596, <https://doi.org/10.1029/2001GL014562>, 2002.
- 30 Anderson, D., Anghel, A., Chau, J., and Veliz, O.: Daytime vertical $E \times B$ drift velocities inferred from ground-based magnetometer observations at low latitudes, *Space Weather*, 2, 2004.
- Anderson, D., Anghel, A., Chau, J. L., and Yumoto, K.: Global, low-latitude, vertical $E \times B$ drift velocities inferred from daytime magnetometer observations, *Space Weather*, 4, 2006.
- 35 Arikani, F., Nayir, H., Sezen, U., and Arikani, O.: Estimation of single station interfrequency receiver bias using GPS-TEC, *Radio Science*, 43, 2008.
- Basu, S. and Basu, S.: Equatorial scintillations-A review, *Journal of Atmospheric and Terrestrial Physics*, 43, 473–489, 1981.

- Basu, S., MacKenzie, E., and Basu, S.: Ionospheric constraints on VHF/UHF communications links during solar maximum and minimum periods.
- Basu, S., MacKenzie, E., and Basu, S.: Ionospheric constraints on VHF/UHF communications links during solar maximum and minimum periods, *Radio Science*, 23, 363–378, 1988.
- 5 Basu, S., Kudeki, E., Basu, S., Valladares, C., Weber, E., Zengingonul, H., Bhattacharyya, S., Sheehan, R., Meriwether, J., Biondi, M., Kuenzler, H., and Espinoza, J.: Scintillations, plasma drifts, and neutral winds in the equatorial ionosphere after sunset, *J. Geophys Res*, 101, 26795-26809, 1996.
- Batista, I., Abdu, M., and Bittencourt, J.: Equatorial F region vertical plasma drifts: Seasonal and longitudinal asymmetries in the American sector, *Journal of Geophysical Research: Space Physics*, 91, 12 055–12 064, 1986.
- 10 Bhattacharyya, A., Beach, T., Basu, S., and Kintner, P.: Nighttime equatorial ionosphere: GPS scintillations and differential carrier phase fluctuations, *Radio Science*, 35, 209–224, 2000.
- Biktash, L.: Role of the magnetospheric and ionospheric currents in the generation of the equatorial scintillations during geomagnetic storms, in: *Annales Geophysicae*, vol. 22, pp. 3195–3202, Copernicus GmbH, 2004.
- Bolaji, O., Adebisi, S., and Fashae, J.: Characterization of ionospheric irregularities at different longitudes during quiet and disturbed geo-
- 15 magnetic conditions, *Journal of Atmospheric and Solar-Terrestrial Physics*, 182, 93–100, 2019.
- Burke, W. J., Gentile, L. C., Huang, C. Y., Valladares, C. E., and Su, S. Y.: Longitudinal variability of equatorial plasma bubbles observed by DMSP and ROCSAT-1, *J. Geophys. Res.*, 19, <https://doi.org/10.1029/2004JA010583>, 2004.
- Cesaroni, C., Spogli, L., Alfonsi, L., De Franceschi, G., Ciraolo, L., Monico, J. F. G., Scotto, C., Romano, V., Aquino, M., and Bougard, B.: L-band scintillations and calibrated total electron content gradients over Brazil during the last solar maximum, *Journal of Space Weather*
- 20 and Space Climate, 5, A36, 2015.
- Chu, F., Liu, J.Y., a. T. H., Sobral, J., Taylor, M., and Medeiros, A. F.: The climatology of ionospheric plasma bubbles and irregularities over Brazil, *Annales Geophysical*, 23: 379-384, 2005.
- Crain, D., Heelis, R., and Bailey, G.: Effects of electrical coupling on equatorial ionospheric plasma motions: When is the F region a dominant driver in the low-latitude dynamo?, *Journal of Geophysical Research: Space Physics*, 98, 6033–6037, 1993.
- 25 Dabas, R., Singh, L., Lakshmi, D., Subramanyam, P., Chopra, P., and Garg, S.: Evolution and dynamics of equatorial plasma bubbles: Relationships to ExB drift, postsunset total electron content enhancements, and equatorial electrojet strength, *Radio Science*, 38, 2003a.
- Dabas, R. S., Singh, L., Lakshmi, D. R., Subramanyam, P., Chopra, P., and Garg, S. C.: Evolution and dynamics of equatorial plasma bubbles: Relationships to ExB drift, postsunset total electron content enhancements, and equatorial electrojet strength., *Radio Sci.*, 38(4), 1075, <https://doi.org/10.1029/2001RS002586>., 2003b.
- 30 Dasgupta, A., Anderson, D., and Klobuchar, J.: Equatorial F-region ionization differences between March and September, *Adv. Space Res.*, 10, 199-202, 1983.
- Dubazane, M. B. and Habarulema, J. B.: An empirical model of vertical plasma drift over the African sector, *Space Weather*, 16, 619–635, 2018.
- Dugassa, T., Habarulema, J. B., and Nigussie, M.: Longitudinal variability of occurrence of ionospheric irregularities over the American,
- 35 African and Indian regions during geomagnetic storms, *Advances in Space Research*, 2019.
- Eccles, J. V.: Modeling investigation of the evening prereversal enhancement of the zonal electric field in the equatorial ionosphere, *Journal of Geophysical Research: Space Physics*, 103, 26 709–26 719, 1998.

- Echer, E., Tsurutani, B., and Gonzalez, W.: Interplanetary origins of moderate ($-100 \text{ nT} < \text{Dst} < -50 \text{ nT}$) geomagnetic storms during solar cycle 23 (1996–2008), *Journal of Geophysical Research: Space Physics*, 118, 385–392, 2013.
- Farley, D., Balsey, B., Woodman, R., and McClure, J.: Equatorial spread F: Implications of VHF radar observations, *Journal of Geophysical Research*, 75, 7199–7216, 1970.
- 5 Farley, D., Bonelli, E., Fejer, B. G., and Larsen, M.: The prereversal enhancement of the zonal electric field in the equatorial ionosphere, *Journal of Geophysical Research: Space Physics*, 91, 13 723–13 728, 1986a.
- Farley, D., Bonelli, E., Fejer, B. G., and Larsen, M.: The prereversal enhancement of the zonal electric field in the equatorial ionosphere, *Journal of Geophysical Research: Space Physics*, 91, 13 723–13 728, 1986b.
- Fejer, B.: Low latitude electrodynamic plasma drifts: a review., *J. Atmos. Terr. Phys.*, 53, 677–693, 1991.
- 10 Fejer, B., Jensen, J., and Su, S.: Quiet time equatorial F region vertical plasma drift model derived from ROCSAT-1 observations., *J. Geophys. Res.*, <https://doi.org/http://dx.doi.org/10.1029/2007JA012801>., 2008.
- Fejer, B. G.: Low latitude ionospheric electrodynamic, *Space Science Reviews*, 158, 145–166, 2011.
- Fejer, B. G., Scherliess, L., and de Paula, E. R.: Effects of the vertical plasma drift velocity on the generation and evolution of equatorial spread F, *J. Geophys. Res.*, 104, 19,859–19,869, <https://doi.org/10.1029/1999JA900271>, 1999.
- 15 Foster, J.: Quantitative investigation of ionospheric density gradients at mid latitudes, in: *Proceedings of the Institute of Navigation ION 2000 Conference*, 2000.
- Haerendel, G. and Eccles, J.: The role of the equatorial electrojet in the evening ionosphere, *Journal of Geophysical Research: Space Physics*, 97, 1181–1192, 1992.
- Hajra, R., Chakraborty, S., Mazumdar, S., and Alex, S.: Evolution of equatorial irregularities under varying electrodynamic conditions: a
- 20 multitechnique case study from Indian longitude zone, *Journal of Geophysical Research: Space Physics*, 117, 2012.
- Heelis, R., Kendall, P., Moffett, R., Windle, D., and Rishbeth, H.: Electrical coupling of the E-and F-regions and its effect on F-region drifts and winds, *Planetary and Space Science*, 22, 743–756, 1974.
- Horvath, I. and Essex, E.: Vertical $E \times B$ drift velocity variations and associated low-latitude ionospheric irregularities investigated with the TOPEX and GPS satellite data, in: *Annales Geophysicae*, vol. 21, pp. 1017–1030, 2003.
- 25 Hua, H. W. C. Y. S. and Chunbo, Z.: Study of Ionospheric TEC Horizontal Gradient by Means of GPS Observations [J], *Chinese Journal of Space Science*, 2, 2009.
- Hysell, D. and Burcham, J.: Ionospheric electric field estimates from radar observations of the equatorial electrojet, *Journal of Geophysical Research: Space Physics*, 105, 2443–2460, 2000.
- Iyer, K., Souza, J., Pathan, B., Abdu, M., Jivani, M., and Joshi, H.: A model of equatorial and low latitude VHF scintillation in India, *Indian*
- 30 *J. Radio Space Phys.*, 35, 98–104., 2006.
- Jakowski, N., Leitinger, R., and Ciruolo, L.: Behaviour of large scale structures of the electron content as a key parameter for range errors in GNSS applications, *Annals of Geophysics*, 47, 2004.
- Jakowski, N., Stankov, S., and Klaehn, D.: Operational space weather service for GNSS precise positioning, in: *Annales Geophysicae*, vol. 23, pp. 3071–3079, 2005.
- 35 Kassa, T. and Damtie, B.: Ionospheric irregularities over Bahir Dar, Ethiopia during selected geomagnetic storms, *Advances in Space Research*, 60, 121–129, 2017.
- Kelley, M.: *The Earth's Ionosphere: Plasma Physics and Electrodynamics*, London, 1989.

- Kelley, M., Ilma, R. R., and Crowley, G.: On the origin of pre-reversal enhancement of the zonal equatorial electric field, *Ann. Geophys*, 27, 2053-2056, 2009.
- Kelley, M. C.: *The Earth's ionosphere: plasma physics and electrodynamics*, vol. 96, Academic press, 2009.
- Kintner, P., Ledvina, B., and Paula, E.: GPS and ionospheric scintillations, *Space Weather*, 5, S09003,
5 <https://doi.org/http://dx.doi.org/10.1029/2006SW000260>, 2007.
- Lee, J., Pullen, S., Datta-Barua, S., and Enge, P.: Assessment of ionosphere spatial decorrelation for global positioning system-based aircraft landing systems, *Journal of Aircraft*, 44, 1662–1669, 2007.
- Lee, J., Datta-Barua, S., Zhang, G., Pullen, S., and Enge, P.: Observations of low-elevation ionospheric anomalies for ground-based augmentation of GNSS, *Radio Science*, 46, 2011.
- 10 Lee, J. H., Pullen, S., Datta-Barua, S., and Enge, P.: Assessment of nominal ionosphere spatial decorrelation for laas, in: 2006 IEEE/ION Position, Location, And Navigation Symposium, 2010.
- Loewe, C. A. and Pröls, G. W.: Classification and mean behavior of magnetic storms, *Journal of Geophysical Research: Space Physics*, 102, 14 209–14 213, 1997.
- Luo, M., Pullen, S., Akos, D., Xie, G., Datta-Barua, S., Walter, T., and Enge, P.: Assessment of ionospheric impact on LAAS using WAAS
15 supertruth data, in: *Proceedings of The ION 58th Annual Meeting*, pp. 24–26, Citeseer, 2002.
- Ma, G. and Maruyama, T.: A super bubble detected by dense GPS network at East Asian longitudes., *Geophys. Res. Lett.*, 133, L21103, 2006.
- Magdaleno, S., Herraiz, M., Altadill, D., and Benito, A.: Climatology characterization of equatorial plasma bubbles using GPS data, *Journal of Space Weather and Space Climate*, 7, A3, 2017.
- 20 Manju, G., e. a.: Equinoctial asymmetry in the occurrence of equatorial spread-F over Indian longitudes during moderate to low solar activity period., *Indian J. Radio Space Phys.*, 41, 240-246, 2013.
- Manju, G. and Haridas, M. M.: On the equinoctial asymmetry in the threshold height for the occurrence of equatorial spread F, *J. Atmos. Sol.Terr. Phys.*, 124, 59-62, 2015a.
- Manju, G. and Haridas, M. M.: On the equinoctial asymmetry in the threshold height for the occurrence of equatorial spread F, *Journal of*
25 *Atmospheric and Solar-Terrestrial Physics*, 124, 59–62, 2015b.
- Manju, G., Devasia, C., and Ravindran, S.: The seasonal and solar cycle variations of electron density gradient scale length, vertical drift and layer height during magnetically quiet days: Implications for Spread F over Trivandrum, India, Earth, planets and space, 61, 1339–1343, 2009.
- Manju, G., Haridas, M., Ravindran, S., Pant, T. K., and Ram, S. T.: Equinoctial asymmetry in the occurrence of equatorial spread-F over
30 Indian longitudes during moderate to low solar activity period 2004-2007, 94.20. dt; 94.20. Vv; 96.60. qd, 2012.
- Manoj, C. and Maus, S.: A real-time forecast service for the ionospheric equatorial zonal electric field, *Space Weather*, 10, 2012.
- Martinis, C. R., Mendillo, M. J., and Aarons, J.: Toward a synthesis of equatorial spread F onset and suppression during geomagnetic storms, *J. Geophys. Res.*, 110, A07306, <https://doi.org/10.1029/2003JA010362>, 2005.
- Maruyama, T., Saito, S., Kawamura, M., Nozaki, K., Krall, J., and Huba, J.: Equinoctial asymmetry of a low-latitude ionosphere-
35 thermosphere system and equatorial irregularities: evidence for meridional wind control, in: *Annales geophysicae*, vol. 27, pp. 2027–2034, Copernicus GmbH, 2009.
- Mendillo, M., Lin, B., and Aarons, J.: The application of GPS observations to equatorial aeronomy., *Radio Sci.*, 35, 885-904., 2000.

- Mendillo, M., Meriwether, J., and Biondi, M.: Testing the thermospheric neutral wind suppression mechanism for day-to-day variability of equatorial spread F., *J. Geophys. Res.*, 106, 3655., 2001.
- Muella, M., De Paula, E., Kantor, I., Batista, I., Sobral, J., Abdu, M., Kintner, P., Groves, K., and Smorigo, P.: GPS L-band scintillations and ionospheric irregularity zonal drifts inferred at equatorial and low-latitude regions, *Journal of Atmospheric and Solar-Terrestrial Physics*, 5 70, 1261–1272, 2008.
- Mungufeni, P., Jurua, E., Habarulema, J., and Anguma, S.: Modelling the probability of ionospheric irregularity occurrence over African low latitude region., *J. Atmos. Solar Terr. Phys.*, 128, 46-57, 2015.
- Mungufeni, P., Jurua, E., and Habarulema, J.: Trends of ionospheric irregularities over African low latitude region during quiet geomagnetic conditions., *J. Atmos. Solar Terr. Phys.*, 138-139, 261-267, <https://doi.org/http://dx.doi.org/10.1016/j.jastp.2016.01.015>, 2016.
- 10 Mushini, S. C., P. T. J. R. B. L. J. W. M. and Pokhotelov, D.: Improved amplitude and phase scintillation indices derived from wavelet detrended high latitude GPS data, *PS Solut.*, <https://doi.org/10.1007/s10291-011-0238-4>, 2011.
- Nava, B., Radicella, S., Leitinger, R., and Coisson, P.: Use of total electron content data to analyze ionosphere electron density gradients, *Advances in Space Research*, 39, 1292–1297, 2007.
- Nayak, C., Tsai, L.-C., Su, S.-Y., Galkin, I., Caton, R., and Groves, K.: Suppression of ionospheric scintillation during St. Patrick's Day 15 geomagnetic super storm as observed over the anomaly crest region station Pingtung, Taiwan: A case study, *Advances in Space Research*, 60, 396-405, <https://doi.org/http://dx.doi.org/10.1016/j.asr.2016.11.036>, 2017.
- Ngwira, C. M., Klenzing, J., Olwendo, J., D'ujanga, F. M., Stoneback, R., and Baki, P.: A study of intense ionospheric scintillation observed during a quiet day in the East African low-latitude region, *Radio Sci.*, 48, 396-405., <https://doi.org/10.1002/rds.20045>, 2013.
- Nishioka, M., Saito, A., and Tsugawa, T.: Occurrence characteristics of plasma bubble derived from global ground-based GPS receiver 20 networks, *J. Geophys. Res.*, 113, A05301, <https://doi.org/10.1029/2007JA012605>, 2008.
- Oladipo, O. A. and Schuler, T.: Magnetic storm effect on the occurrence of ionospheric irregularities at an equatorial station in the African sector, *Ann.Geophys.*, 56, 5, A0565, <https://doi.org/10.4401/ag-6247>, 2013a.
- Oladipo, O. A. and Schuler, T.: Equatorial ionospheric irregularities using GPS TEC derived index., *Atmos. Sol. Terr. Phys.*, 92, 78-82., 2013b.
- 25 Oladipo, O. A., Adeniyi, J. O., Olawepo, A. O., and Doherty, P. H.: Large-scale ionospheric irregularities occurrence at Ilorin, Nigeria, *Space Weather.*, 12, 300-305., <https://doi.org/10.1002/2013SW000991>, 2014.
- Olwendo, J., Cilliers, P., Weimin, Z., Ming, O., and Yu, X.: Validation of ROTI index for ionospheric amplitude scintillation measurements in a low latitude region over Africa., *Radio Science*, 2018.
- Olwendo, O., Baluku, T., Baki, P., Cilliers, P., Mito, C., and Doherty, P.: Low latitude ionospheric scintillation and zonal irregular- 30 ity drifts observed with GPS-SCINDA system and closely spaced VHF receivers in Kenya, *Adv. in Space Res.*, 51, 1715-1726., <https://doi.org/http://dx.doi.org/10.1016/j.asr.2012.12.017>, 2013.
- Olwendo, O., Baki, P., Cilliers, P., Doherty, P., and Radicella, S.: Low latitude ionospheric scintillation and zonal plasma irregularity drifts climatology around the equatorial anomaly crest over Kenya, *J. Atmo. Solar-Terr. Phys.*, 138-139, 9-22., 2016.
- Otsuka, Y., Shiokawa, K., and Ogawa, T.: Equatorial ionospheric scintillations and zonal irregularity drifts observed with closely spaced GPS 35 receivers in Indonesia., *J. Meteorol. Soc. Jpn.*, 84A, 343-351, 2006.
- Otsuka, Y., Ogawa, T., et al.: VHF radar observations of nighttime F-region field-aligned irregularities over Kototabang, Indonesia, *Earth, planets and space*, 61, 431–437, 2009.

- Paznukhov, V., Carrano, C., Doherty, P., Groves, K., Caton, R.G., a. V. C., Seemala, G., Bridgwood, C., Adeniyi, J., Amaeshi, L., Dامتie, B., a. D. M. F., Ndeda, J., Baki, P., Obrou, O., Okere, B., and Tsidu, G.: Equatorial plasma bubbles and L-band scintillations in Africa during solar minimum., *Ann. Geophys.*, 30, 675-682, 2012.
- Pi, X., Mannucci, A. J., Lindqwister, U. J., and Ho, C.: Monitoring of Global Ionospheric Irregularities using the worldwide GPS, *Geophys. Res. Lett.*, 24, 2283-2286, <https://doi.org/10.1029/97GL02273>, 1997.
- Pradipta, R. and Doherty, P. H.: Assessing the occurrence pattern of large ionospheric TEC gradients over the Brazilian airspace, *Navigation: Journal of The Institute of Navigation*, 63, 335-343, 2016.
- Radicella, S. M., Nava, B., Coisson, P., Kersley, L., and Bailey, G. J.: Effects of gradients of the electron density on Earth-space communications, *Annals of Geophysics*, 47, 2004.
- 10 Ram, S. T., Rao, P. R., Prasad, D., Niranjan, K., Babu, A. R., Sridharan, R., Devasia, C., and Ravindran, S.: The combined effects of electrojet strength and the geomagnetic activity (Kp-index) on the post sunset height rise of the F-layer and its role in the generation of ESF during high and low solar activity periods, *Ann. Geophys.*, 25, 2007.
- Rao, P. R., Krishna, S. G., Niranjan, K., and Prasad, D.: Study of spatial and temporal characteristics of L-band scintillations over the Indian low-latitude region and their possible effects on GPS navigation, in: *Annales Geophysicae*, vol. 24, pp. 1567-1580, 2006a.
- 15 Rao, P. R., Krishna, S. G., Niranjan, K., and Prasad, D.: Study of spatial and temporal characteristics of L-band scintillations over the Indian low-latitude region and their possible effects on GPS navigation, in: *Annales Geophysicae*, vol. 24, pp. 1567-1580, 2006b.
- Rao, P. R., Krishna, S. G., Niranjan, K., and Prasad, D.: Temporal and spatial variations in TEC using simultaneous measurements from the Indian GPS network of receivers during the low solar activity period of 2004-2005, in: *Annales Geophysicae*, vol. 24, pp. 3279-3292, 2006c.
- 20 Rastogi, R. and Woodman, R.: Spread F in equatorial ionograms associated with reversal of horizontal F region electric field, in: *Annales de Geophysique*, vol. 34, pp. 31-36, 1978.
- Rastogi, R., Kitamura, T., and Kitamura, K.: Geomagnetic field variations at the equatorial electrojet station in Sri Lanka, Peredinia, in: *Annales Geophysicae*, vol. 22, pp. 2729-2739, 2004.
- Rastogi, R. G. and Klobuchar, J. A.: Ionospheric electron content within the equatorial F2 layer anomaly belt., *J. Geophys. Res.*, 25 95(A11),19,045-19,052, 1990.
- Ratnam, D. V., Vishnu, T. R., and Harsha, P. B. S.: Ionospheric Gradients Estimation and Analysis of S-Band Navigation Signals for NAVIC System, *IEEE Access*, 6, 66 954-66 962, 2018.
- Ravi Chandra, K., Satya Srinivas, V., and Sarma, A.: Investigation of ionospheric gradients for GAGAN application, Earth, planets and space, 61, 633-635, 2009.
- 30 Ray, S., Paul, A., and Dasgupta, A.: Equatorial scintillations in relation to the development of ionization anomaly, in: *Annales Geophysicae*, vol. 24, pp. 1429-1442, 2006.
- Rishbeth, H.: Polarization fields produced by winds in the equatorial F-region, *Planetary and Space Science*, 19, 357-369, 1971a.
- Rishbeth, H.: Polarization fields produced by winds in the equatorial F-region, *Planetary and Space Science*, 19, 357-369, 1971b.
- Rungraengwajjake, S., Supnithi, P., Saito, S., Siansawasdi, N., and Saekow, A.: Ionospheric delay gradient monitoring for GBAS by GPS stations near Suvarnabhumi airport, Thailand., *Radio Sci.*, 50, 1076-1085, <https://doi.org/10.1002/2015RS005738>, 2015a.
- 35 Rungraengwajjake, S., Supnithi, P., Saito, S., Siansawasdi, N., and Saekow, A.: Ionospheric delay gradient monitoring for GBAS by GPS stations near Suvarnabhumi airport, Thailand, *Radio Science*, 50, 1076-1085, 2015b.

- Saito, S. and Yoshihara, T.: Evaluation of extreme ionospheric total electron content gradient associated with plasma bubbles for GNSS Ground-Based Augmentation System, *Radio Science*, 52, 951-962, 2017.
- Sardón, E. and Zarraoa, N.: Estimation of total electron content using GPS data: How stable are the differential satellite and receiver instrumental biases?, *Radio science*, 32, 1899–1910, 1997.
- 5 Scherliess, L. and Fejer, B.: Radar and satellite global equatorial F region vertical drift model, *J. Geophys. Res.*, 104 (4A), 6829-6842, 1999.
- Seba, E. and Nigussie, M.: Investigating the effect of geomagnetic storm and equatorial electrojet on equatorial ionospheric irregularity over East African sector., *Adv. Space Res.*, 58,1708–1719, 2016.
- Seba, E. and Tsegaye, K. G.: Characterization of ionospheric scintillation at a geomagnetic equatorial region station., *Adv. Space Res.*, 56, 2057-2063, 2015.
- 10 Seba, E. B., Nigussie, M., and Moldwin, M. B.: The relationship between equatorial ionization anomaly and nighttime equatorial spread F in East Africa, *Advances in Space Research*, 62, 1737–1752, 2018.
- Seemala, G. and Valladares, C.: Statistics of total electron content depletions observed over the South American continent for the year 2008, *Radio Science*, 46, RS5019, 2011.
- Sreeja, V., Devasia, C., Ravindran, S., and Pant, T. K.: Observational evidence for the plausible linkage of Equatorial Electrojet (EEJ) electric field variations with the post sunset F-region electrodynamics, in: *Annales geophysicae: atmospheres, hydrospheres and space sciences*, vol. 27, p. 4229, 2009.
- 15 Sripathi, S., Kakad, B., and Bhattacharyya, A.: Study of equinoctial asymmetry in the Equatorial Spread F (ESF) irregularities over Indian region using multi-instrument observations in the descending phase of solar cycle 23, *J. Geophys. Res.*, 116, A11302, <https://doi.org/10.1029/2011JA016625>., 2011.
- 20 Sun, Y.-Y., Matsuo, T., Araujo-Pradere, E. A., and Liu, J.-Y.: Ground-based GPS observation of SED-associated irregularities over CONUS, *Journal of Geophysical Research: Space Physics*, 118, 2478–2489, 2013.
- Susnik, A. and Forte, B.: Ionospheric scintillation activity measured in the African sector, paper presented at General Assembly and Scientific Symposium, XXXth URSI, Istanbul, Turkey., 2011.
- Taabu, S., D’ujanga, F., and Ssenyonga, T.: Prediction of ionospheric scintillation using neural network over East African region during ascending phase of sunspot cycle 24, *Adv. Space Res.*, <https://doi.org/http://dx.doi.org/10.1016/j.asr.2016.01.014>, 2016.
- 25 Takahashi, H., Wrasse, C., Denardini, C., Pádua, M., de Paula, E., Costa, S., Otsuka, Y., Shiokawa, K., Monico, J. G., Ivo, A., et al.: Ionospheric TEC weather map over South America, *Space Weather*, 14, 937–949, 2016.
- Tsunoda, R.: Control of the seasonal and longitudinal occurrence of equatorial scintillations by the longitudinal gradient in integrated E region Pederson conductivity., *J. Geophys. Res.*, 90, 447., 1985.
- 30 Tsunoda, R. T.: On the enigma of day-to-day variability in Wave structure in equatorial Spread F, *Geophys. Res. Lett.*, 32, 2005.
- Tsunoda, R. T.: On seeding equatorial spread F during solstices, *Geophysical Research Letters*, 37, 2010.
- Tulasi Ram, S., Rao, P. V. S. R., Niranjana, K., Prasad, D. S. V. V. D., Sridharan, R., Devasia, C. V., and Ravindran, S.: The role of post-sunset vertical drifts at the equator in predicting the onset of VHF scintillations during high and low sunspot activity years., *Ann. Geophys.*, 24, 1609-1616, 2006.
- 35 Uemoto, J., Maruyama, T., Saito, S., Ishii, M., and Yoshimura, R.: Relationships between pre-sunset electrojet strength, pre-reversal enhancement and equatorial spread-F onset., *Annales Geophysicae (09927689)*, 28, 2010.
- Valladares, C., Basu, S., Groves, K., Hagan, M., Hysell, D., Mazzella Jr., A., and Sheehan, R.: Measurement of the latitudinal distribution of total electron content during equatorial spread-F events, *J. Geophys. Res.*, 106, 29133-29152, 2001.

- Valladares, C., Villalobos, J., Sheehan, R., and Hagan, M.: Latitudinal extension of low-latitude scintillations measured with a network of GPS receivers, *Ann. Geophys.*, 22, 3155-3175, 2004.
- Wathanasangmechai, K., Yamamoto, M., Saito, A., Tsunoda, R., Yokoyama, T., Supnithi, P., Ishii, M., and Yatini, C.: Predawn plasma bubble cluster observed in Southeast Asia, *Journal of Geophysical Research: Space Physics*, 121, 5868–5879, 2016.
- 5 Wernik, A. and Liu, C.: Ionospheric irregularities causing scintillation of GHz frequency radio signals, *Journal of Atmospheric and Terrestrial Physics*, 36, 871–879, 1974.
- Whalen, J. A.: The equatorial anomaly: Its quantitative relation to equatorial bubbles, bottomside spread F, and $E \times B$ drift velocity during a month at solar maximum, *Journal of Geophysical Research: Space Physics*, 106, 29 125–29 132, 2001.
- Wiens, R. H., Ledvina, B. M., a. K. P. M., Afewerki, M., and Mulugheta, Z.: Equatorial plasma bubbles in the ionosphere over Eritrea: Occurrence and drift speed, *Ann. Geophys.*, 24, 1443–1453, 2006.
- 10 Woodman, R.: Vertical drift velocities and East-West electric fields at the magnetic equator., *J. Geophys. Res.*, 75(31), 6249-6259, <https://doi.org/10.1029/JA075i031p06249>, 1970.
- Yizengaw, E. and Moldwin, M. B.: African Meridian B-field Education and Research (AMBER) array., *Earth Moon Planet*, 104, 237-246, <https://doi.org/10.1007/s11038-008-9287-2>, 2009.
- 15 Yizengaw, E., Moldwin, M. B., Mebrahtu, A., Damtie, B., Zesta, E., Valladares, C. E., and Doherty, P.: Comparison of storm time equatorial ionospheric electrodynamic in the African and American sectors, *J. Atmos. Sol.-Terr. Phys.*, 73(1), 156–163, <https://doi.org/10.1016/j.jastp.2010.08.008>., 2011.
- Yizengaw, E., Zesta, E., a. M. M. B., Damtie, B., Mebrahtu, A., Valladares, C. E., and Pfaff, R. F.: Longitudinal differences of ionospheric vertical density distribution and equatorial electrodynamic., *J. Geophys. Res.*, 117, A07312, <https://doi.org/10.1029/2011JA017454>.,
- 20 2012.
- Yizengaw, E., Moldwin, M. B., Zesta, E. and Biouele, C. M., Damtie, B., Mebrahtu, A., Rabiou, B., Valladares, C. F., and Stoneback, R.: The longitudinal variability of equatorial electrojet and vertical drift velocity in the African and American sectors., *Ann. Geophys.*, 32, 231-238, 2014.
- Yoshihara, T., Sakai, T., Fujii, N., and Saitoh, A.: An investigation of local-scale spatial gradient of ionospheric delay using the nation-wide GPS network data in Japan, in: ION National Technical Meeting, San Diego, CA, 2005.
- 25